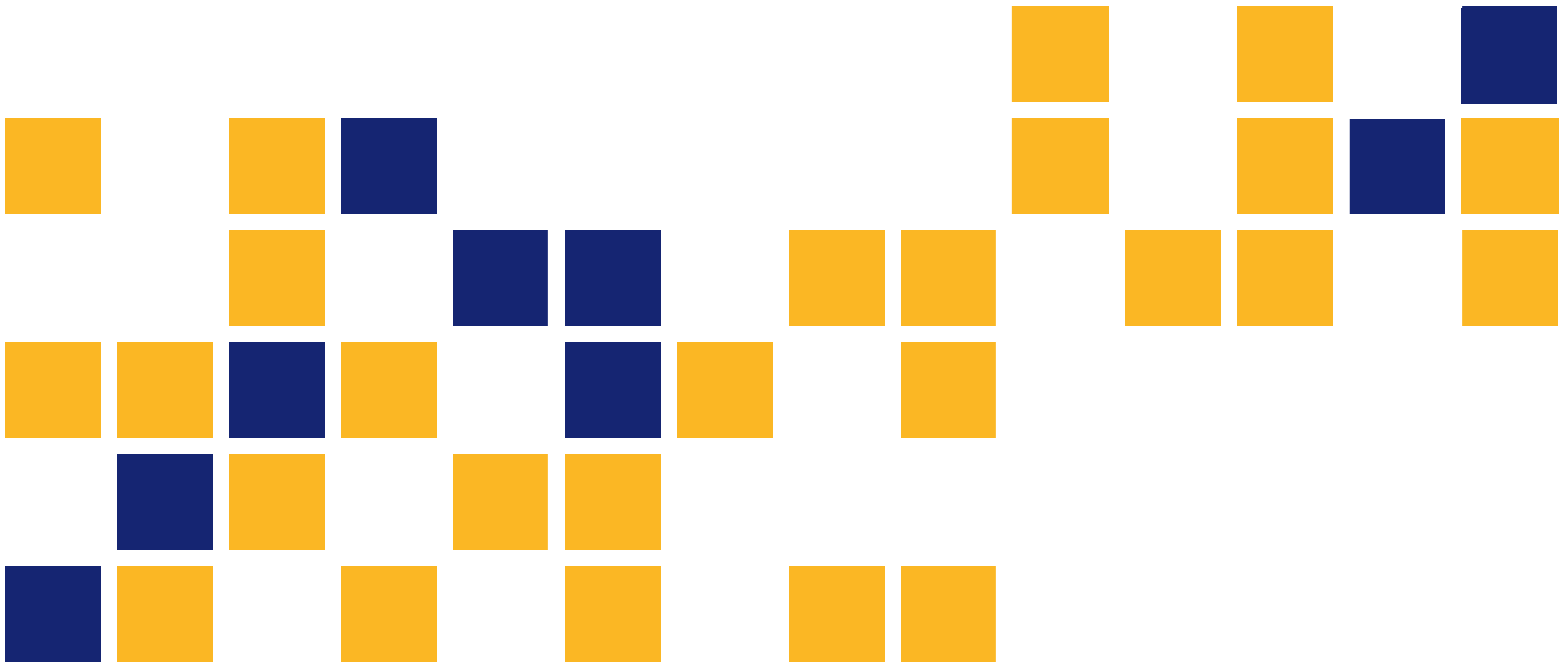


Testing Aggregate Backfill for Corrosion Potential

Zachary Brady
Robert Parsons, Ph.D., P.E.
Jie Han, Ph.D., P.E.

The University of Kansas



| | | | |
|---|--|--|-----------------|
| 1 Report No. K-TRAN: KU-15-5 | 2 Government Accession No. | 3 Recipient Catalog No. | |
| 4 Title and Subtitle Testing Aggregate Backfill for Corrosion Potential | | 5 Report Date March 2016 | |
| | | 6 Performing Organization Code | |
| 7 Author(s) Zachary Brady, Robert Parsons, Ph.D., P.E., Jie Han, Ph.D., P.E. | | 7 Performing Organization Report No. | |
| 9 Performing Organization Name and Address The University of Kansas Department of Civil, Environmental and Architectural Engineering 1530 West 15th St Lawrence, Kansas 66045-7609 | | 10 Work Unit No. (TRAIS) | |
| | | 11 Contract or Grant No. C2035 | |
| 12 Sponsoring Agency Name and Address Kansas Department of Transportation Bureau of Research 2300 SW Van Buren Topeka, Kansas 66611-1195 | | 13 Type of Report and Period Covered Final Report August 2014–October 2015 | |
| | | 14 Sponsoring Agency Code RE-0663-01 | |
| 15 Supplementary Notes For more information write to address in block 9. | | | |
| <p>The Kansas Department of Transportation (KDOT) has designed and constructed numerous mechanically stabilized earth (MSE) walls to support new and expanded highway projects throughout Kansas. MSE walls often contain galvanized steel strips as the mechanical reinforcement within layers of specified backfill material. Inclusion of these strips creates a stronger composite material connected to a visually appealing wall facing, but galvanized steel reinforcement is potentially vulnerable to corrosion.</p> <p>Corrosivity of MSE backfill is typically characterized using electrical resistivity among other properties. KDOT currently uses the American Association of State Highway and Transportation Officials (AASHTO) Standard T 288 (2012) to calculate the resistivity of MSE backfill. There is concern that this method may not reflect field conditions well, and thus may mischaracterize the corrosivity of backfill. AASHTO T 288 tests were conducted as a part of this research, and the condition of the samples at the time of testing was not consistent with expected field conditions.</p> <p>A new procedure has been proposed that appears to more accurately simulate field conditions. This new procedure (ASTM C XXX-XX) has been extensively tested and compared with AASHTO T 288 in this experimental study. The proposed ASTM test simulated expected field conditions more accurately than the AASHTO T 288 test. Results also appear to indicate the need for a larger resistivity box to accurately characterize the corrosivity of larger aggregates. Preliminary recommendations for box geometry are 8:1 minimum electrode spacing to maximum particle size and 3:1 minimum height to maximum particle size. It was also observed that increasing the number of soak/drain cycles of the material resulted in a substantial increase in resistivity.</p> | | | |
| 17 Key Words Corrosion, Electrical Resistivity, Mechanically Stabilized Earth, Aggregate Backfill | | 18 Distribution Statement No restrictions. This document is available to the public through the National Technical Information Service www.ntis.gov . | |
| 19 Security Classification (of this report) Unclassified | 20 Security Classification (of this page) Unclassified | 21 No. of pages 70 | 22 Price |

Form DOT F 1700.7 (8-72)

This page intentionally left blank.

Testing Aggregate Backfill for Corrosion Potential

Final Report

Prepared by

Zachary Brady
Robert Parsons, Ph.D., P.E.
Jie Han, Ph.D., P.E.

The University of Kansas

A Report on Research Sponsored by

THE KANSAS DEPARTMENT OF TRANSPORTATION
TOPEKA, KANSAS

and

THE UNIVERSITY OF KANSAS
LAWRENCE, KANSAS

March 2016

© Copyright 2016, **Kansas Department of Transportation**

PREFACE

The Kansas Department of Transportation's (KDOT) Kansas Transportation Research and New-Developments (K-TRAN) Research Program funded this research project. It is an ongoing, cooperative and comprehensive research program addressing transportation needs of the state of Kansas utilizing academic and research resources from KDOT, Kansas State University and the University of Kansas. Transportation professionals in KDOT and the universities jointly develop the projects included in the research program.

NOTICE

The authors and the state of Kansas do not endorse products or manufacturers. Trade and manufacturers names appear herein solely because they are considered essential to the object of this report.

This information is available in alternative accessible formats. To obtain an alternative format, contact the Office of Public Affairs, Kansas Department of Transportation, 700 SW Harrison, 2nd Floor – West Wing, Topeka, Kansas 66603-3745 or phone (785) 296-3585 (Voice) (TDD).

DISCLAIMER

The contents of this report reflect the views of the authors who are responsible for the facts and accuracy of the data presented herein. The contents do not necessarily reflect the views or the policies of the state of Kansas. This report does not constitute a standard, specification or regulation.

Abstract

The Kansas Department of Transportation (KDOT) has designed and constructed numerous mechanically stabilized earth (MSE) walls to support new and expanded highway projects throughout Kansas. MSE walls often contain galvanized steel strips as the mechanical reinforcement within layers of specified backfill material. Inclusion of these strips creates a stronger composite material connected to a visually appealing wall facing, but galvanized steel reinforcement is potentially vulnerable to corrosion.

Corrosivity of MSE backfill is typically characterized using electrical resistivity among other properties. KDOT currently uses the American Association of State Highway and Transportation Officials (AASHTO) Standard T 288 (2012) to calculate the resistivity of MSE backfill. There is concern that this method may not reflect field conditions well, and thus may mischaracterize the corrosivity of backfill. AASHTO T 288 tests were conducted as a part of this research, and the condition of the samples at the time of testing was not consistent with expected field conditions.

A new procedure has been proposed that appears to more accurately simulate field conditions. This new procedure (ASTM C XXX-XX) has been extensively tested and compared with AASHTO T 288 in this experimental study. The proposed ASTM test simulated expected field conditions more accurately than the AASHTO T 288 test. Results also appear to indicate the need for a larger resistivity box to accurately characterize the corrosivity of larger aggregates. Preliminary recommendations for box geometry are 8:1 minimum electrode spacing to maximum particle size and 3:1 minimum height to maximum particle size. It was also observed that increasing the number of soak/drain cycles of the material resulted in a substantial increase in resistivity.

Acknowledgements

The authors would like to thank the Kansas Department of Transportation (KDOT) and the Kansas Transportation Research And New-Developments Program (K-TRAN) for providing the financial support for the research described in this report; Dr. Stacey Kulesza and Mr. Michael Snapp of Kansas State University for providing field data and technical support for this research; Mr. Jim Brennan of KDOT, Mr. Bill Beggs of Martin Marietta, and Dr. Edward Peltier and Mr. Michael Panethiere, both of The University of Kansas, for providing technical support for this research; Mr. Stephen Lorson of Professional Engineering Consultants (PEC) for providing Pittsburg material field data; Mr. Matthew Maksimowicz, Mr. Kent Dye, and Mr. David Woody of The University of Kansas for their assistance in fabricating the test boxes, and Mr. Madan Neupane and Mr. Jim Jacobe for their assistance with material collection.

Table of Contents

| | |
|--|-----|
| Abstract..... | v |
| Acknowledgements..... | vi |
| Table of Contents..... | vii |
| List of Tables..... | ix |
| List of Figures..... | x |
| Chapter 1: Introduction..... | 1 |
| 1.1 Galvanization Corrosion Process..... | 1 |
| 1.2 MSE Wall Galvanized Steel Reinforcement Design: Electrical Resistivity..... | 2 |
| 1.3 AASHTO T 288 Electrical Resistivity Test Applicability to MSE Wall Backfill..... | 2 |
| Chapter 2: Literature Review..... | 4 |
| 2.1 MSE Wall Overview..... | 4 |
| 2.2 Corrosion Characterization Importance..... | 4 |
| 2.3 Underground (Soil) Corrosion..... | 5 |
| 2.4 MSE Backfill Corrosivity..... | 6 |
| 2.5 Galvanized Steel Anatomy..... | 6 |
| 2.6 Galvanized Steel Reinforcement Corrosion..... | 7 |
| 2.7 Research Directions for MSE Backfill Corrosion Potential Characterization..... | 8 |
| Chapter 3: Research Scope..... | 9 |
| 3.1 Materials Used..... | 9 |
| 3.2 Lab Tests..... | 10 |
| 3.2.1 AASHTO T 288 Soil Electrical Resistivity Test..... | 11 |
| 3.2.2 The New ASTM Aggregate Electrical Resistivity Test..... | 12 |
| Chapter 4: Test Results and Discussion..... | 18 |
| 4.1 AASHTO T 288 Electrical Resistivity..... | 18 |
| 4.1.1 AASHTO T 288 Pittsburg Results..... | 18 |
| 4.1.2 AASHTO T 288 Ridgeview Results..... | 21 |
| 4.1.3 AASHTO T 288 Discussion..... | 22 |
| 4.2 New ASTM Results..... | 23 |
| 4.2.1 SLT Material New ASTM Resistivity Results..... | 28 |
| 4.2.2 Pittsburg Material New ASTM Resistivity Results..... | 29 |
| 4.2.3 Ridgeview Material New ASTM Resistivity Results..... | 30 |

| | |
|---|----|
| 4.2.4 Gray I-70/K-7 New ASTM Resistivity Results SSR8 meter | 33 |
| 4.2.5 Colored I-70/K-7 New ASTM Resistivity Results..... | 34 |
| 4.2.6 New ASTM Testing Parameter Variations Results..... | 35 |
| Chapter 5: Conclusions and Recommendations | 40 |
| 5.1 Conclusions..... | 40 |
| 5.1.1 AASHTO T 288..... | 40 |
| 5.1.2 New ASTM C XXX-XX | 41 |
| 5.1.3 Comparison with Snapp Reported Bulk Field ER..... | 44 |
| 5.2 Recommendations | 44 |
| References..... | 46 |
| Appendix A: Resistivity vs. Geometric Factors Other Than Box Factor | 48 |

List of Tables

Table 3.1: Sample Collection Locations 9

Table 3.2: Sampling Details..... 10

Table 3.3: Material Tests 10

Table 3.4: Electrical Resistivity Box Details 15

Table 4.1: AASHTO T 288 Results (Pittsburg)..... 20

Table 4.2: AASHTO T 288 Results (Ridgeview)..... 22

List of Figures

| | |
|---|----|
| Figure 3.1: AASHTO Electrical Resistivity Box..... | 11 |
| Figure 3.2: AASHTO T 288 Apparatus Setup..... | 12 |
| Figure 3.3: New ASTM Test Boxes Measured Perpendicular to Electrode Plates (Top View)... | 15 |
| Figure 3.4: New ASTM Test Boxes Measured Perpendicular to Electrode Plates (Oblique View)..... | 16 |
| Figure 3.5: NEMA Box Outside (left) and Inside (right) with Threaded Drain Plug..... | 17 |
| Figure 4.1: Grain Size Distributions of Samples from MSE walls..... | 18 |
| Figure 4.2: Filled AASHTO Resistivity Box (Pittsburg, minus No. 10, w = 10 %) | 19 |
| Figure 4.3: Moisture Samples for Each Pittsburg Round (Left: Wet; Right: Dry)..... | 20 |
| Figure 4.4: Moisture Samples for Each Ridgeview Round (Left: Wet; Right: Dry) | 21 |
| Figure 4.5a: All New ASTM Normal Results vs. Box Factor | 24 |
| Figure 4.5b: All New ASTM Normal Results vs. Box Cross-Sectional Area Perpendicular to Electron Flow..... | 25 |
| Figure 4.5c: All New ASTM Normal Results vs. Box Volume | 25 |
| Figure 4.5d: All New ASTM Normal Results vs. Electrode Spacing | 26 |
| Figure 4.5e: All New ASTM Normal Results vs. Electrode Spacing Trends..... | 26 |
| Figure 4.6: SLT New ASTM Results vs. Electrode Spacing..... | 28 |
| Figure 4.7: Pittsburg New ASTM Results vs. Electrode Spacing | 29 |
| Figure 4.8: Ridgeview New ASTM Results vs. Electrode Spacing | 30 |
| Figure 4.9: Ridgeview New ASTM Samples After Soaking and Attempted Draining; AASHTO box (top), Small box (left), and Large box (right)..... | 32 |
| Figure 4.10: Gray I-70/K-7 New ASTM Results vs. Electrode Spacing..... | 33 |
| Figure 4.11: Colored I-70/K-7 New ASTM Results vs. Electrode Spacing..... | 34 |
| Figure 4.12: SLT Resistivity Behavior During and After Draining | 35 |
| Figure 4.13: Pittsburg Cycled Saturated Resistivity vs. Soaking Time in Different Boxes | 36 |
| Figure 4.14: Pittsburg Saturated and Drained Cycled Resistivities vs. Soaking Time in Different Boxes..... | 38 |
| Figure 4.15: Cycled Pittsburg vs. Drained Resistivity..... | 39 |
| Figure 4.16: Cycled Gray I-70/K-7 vs. Drained Resistivity | 39 |
| Figure A.1: New ASTM SLT Resistivity Results vs. Box Factor | 48 |
| Figure A.2: New ASTM SLT Resistivity Results vs. Box Cross Sectional Area | 48 |
| Figure A.3: New ASTM SLT Resistivity Results vs. Box Volume | 49 |

| | |
|---|----|
| Figure A.4: New ASTM Pittsburg Resistivity Results vs. Box Factor..... | 49 |
| Figure A.5: New ASTM Pittsburg Results vs. Box Cross-Sectional Area..... | 50 |
| Figure A.6: New ASTM Pittsburg Results vs. Box Volume | 50 |
| Figure A.7: New ASTM Ridgeview Resistivity Results vs. Box Factor..... | 51 |
| Figure A.8: New ASTM Ridgeview Resistivity Results vs. Box Cross Sectional Area | 51 |
| Figure A.9: New ASTM Ridgeview Resistivity Results vs. Box Volume | 52 |
| Figure A.10: New ASTM Gray I-70/K-7 Resistivity Results vs. Box Factor | 52 |
| Figure A.11: New ASTM Gray I-70/K-7 Resistivity Results vs. Box Cross Sectional Area..... | 53 |
| Figure A.12: New ASTM Gray I-70/K-7 Resistivity Results vs. Box Volume | 53 |
| Figure A.13: New ASTM Colored I-70/K-7 Resistivity Results vs. Box Factor | 54 |
| Figure A.14: New ASTM Colored I-70/K-7 Resistivity Results vs. Box Cross Sectional Area.. | 54 |
| Figure A.15: New ASTM Colored I-70/K-7 Resistivity Results vs. Box Volume..... | 55 |

This page intentionally left blank.

Chapter 1: Introduction

Mechanically stabilized earth (MSE) retaining walls have been used for several decades to support bridge structures, hold excavated slopes in place, and to support new highway and highway widening projects. As MSE wall design developed in the early 1970s, steel was the most popular material used to reinforce soil masses due to its low cost, high strength, and high availability. However, when steel is buried in a soil mass it eventually reverts back to a natural ore-like state. In this case, the refined iron used to make steel will give up its mechanical bond with carbon and other metals in favor of a lower-energy atomic bond with oxygen, which will convert the iron back into its natural iron oxide state. This oxidation reaction causes the iron to rust, or corrode.

1.1 Galvanization Corrosion Process

The consequences of corrosion of metal reinforcement in MSE walls were quickly realized and mitigation procedures were adopted. Almost all steel used to reinforce soil masses is now galvanized, or coated with a layer of pure zinc. The presence of zinc protects the steel in three stages: zinc patina barrier protection, a barrier of protection composed of steel-zinc alloy layers, and cathodic protection. As soon as the galvanization process is complete, the pure zinc layer will begin to react with water in the air. After 6 to 12 months of wet-dry cycles on the pure zinc surface, electrons will have relocated sufficiently to form a much harder patina composed of zinc carbonate, which is insoluble in water and corrodes at $\frac{1}{30}$ th the rate of bare steel in the same environment. As this zinc patina breaks down, the underlying steel-zinc layers will begin to corrode until the bare steel is finally exposed. At this point, cathodic protection takes over, during which the remaining galvanization layers and the bare steel are all in contact with the soil environment. This forms a bimetallic couple, or a galvanic battery cell, in which electrons are transferred from the anode (galvanization layers) to the cathode (bare steel) due to the higher electron affinity of iron. In this way, even though the bare steel is exposed, as long as there is zinc near it, it will not oxidize or corrode. Zinc is also the preferred coating due to its natural occurrence in soil, which eliminates the potential for contamination.

1.2 MSE Wall Galvanized Steel Reinforcement Design: Electrical Resistivity

The corrosion protection offered by galvanization prompted the development of sacrificial galvanization thickness requirements for metal reinforcement based on the corrosivity of the soil used for MSE backfill. The corrosivity of MSE backfill is typically characterized by its electrical resistivity (ER), pH, and organic, sulfates, and chlorides contents. This research focuses on the determination of a material's electrical resistivity, which can be calculated from measurements of apparent resistance in the field or the laboratory. The American Association of State Highway and Transportation Officials (AASHTO) has developed a standard method to measure the apparent electrical resistance of soil using a two-electrode soil box (AASHTO T 288, 2012). The soil box is constructed from chemically fused polycarbonate sheets and has two stainless steel electrode plates connected to opposite interior sides. These plates are connected to exterior stainless steel posts designed to connect to a resistivity meter. Electric current is passed from one electrode through the soil sample to the other electrode, and the resulting voltage difference between the two electrodes is measured. Using Ohm's law, this voltage difference is converted into a measure of resistance in ohms. The resistance is then multiplied by a factor that is a function of box geometry to calculate the electrical resistivity of the material inside the box.

1.3 AASHTO T 288 Electrical Resistivity Test Applicability to MSE Wall Backfill

In recent years, the backfill material used in MSE walls constructed for the Kansas Department of Transportation (KDOT) has shifted from sands to limestone aggregate. Since corrosion is still of significant concern, resistivity testing is still conducted. However, there has been concern that the AASHTO T 288 (2012) test does not accurately provide the true resistivity of the aggregate backfill for several reasons. These reasons include the small size of the AASHTO resistivity box compared with the aggregate particle size. Size is an issue because the box may be too small to allow repeatable laboratory calculations of electrical resistivity for samples containing larger aggregate particle sizes. Also, since the original AASHTO T 288 standard was developed for use with finer-grained soils, there is concern that the procedure used to determine the electrical resistivity of the MSE aggregate backfill does not accurately represent

field conditions of the aggregate, and thus does not give results useful for the design of MSE wall metal reinforcement. This research explores the applicability of the AASHTO T 288 standard to aggregate backfill, the effectiveness of a new ASTM International method to calculate the electrical resistivity of aggregate that better represents MSE wall backfill field conditions, and the approximate size of box required to accurately calculate this aggregate electrical resistivity using the new ASTM International standard method.

The format of the remainder of this report is as follows: Chapter 2 contains a review of the relevant literature; Chapter 3 contains a description of the scope of work of this study, procedures followed, and equipment used; Chapter 4 contains the results of testing and subsequent analysis; and Chapter 5 contains the conclusions and recommendations developed from this study.

Chapter 2: Literature Review

Corrosion of metal reinforcement in MSE walls has been a concern since the earth reinforcement technique was brought to the United States in the 1970s. As larger limestone aggregates have been more widely used as backfill for MSE walls in Kansas, it has become more crucial to characterize their corrosive properties. One of the most important properties of MSE wall backfill is the electrical resistivity, which is currently calculated using AASHTO T 288 (2012). There is concern that AASHTO T 288 may not yield resistivity results that are accurate or repeatable for larger aggregates since the standard was developed for use with finer-grained soils.

Studies have been published regarding characterizing the resistivity of larger aggregates in the laboratory. A summary of selected research is presented in this chapter.

2.1 MSE Wall Overview

The reinforced earth technique, used to build higher and stronger embankments and more stable transportation structures, was developed in pre-1970 France and has since spread worldwide. Layers of metal reinforcement strips or meshes are included within layers of backfill material during construction, and the resulting mass acts as a much stronger composite material. The first, and still very common, reinforcement material used for these structures was galvanized steel, and many mechanically stabilized earth (MSE) walls with steel reinforcement have been built in Kansas.

2.2 Corrosion Characterization Importance

Failure to accurately characterize the corrosivity of a proposed backfill for an MSE wall can have disastrous consequences, especially for walls designed to last up to 75 years. The Nevada Department of Transportation (NDOT) conducted an investigation into accelerated steel reinforcement corrosion within several MSE walls in the Las Vegas metropolitan area. NDOT found that aggregate backfill that was accepted for wall construction in 1985 based on an NDOT standard should have been rejected for MSE use due to its aggressiveness, based on tests conducted during the study. The walls in question were reinforced with nongalvanized welded

wire fabric (Thornley, Siddharthan, Luke, & Salazar, 2010). A separate investigation conducted by an Ohio consulting firm of another retaining wall reinforced with nongalvanized steel revealed several failed tieback anchors within two years after construction due to accelerated corrosion (Esser & Dingeldein, 2007).

Other studies of properly galvanized steel reinforced MSE walls showed lower-than-predicted corrosion of both galvanized and nongalvanized MSE wall pullout coupons in Utah (Billings, 2011) and of galvanized reinforcement samples in Kentucky (Beckham, Sun, & Hopkins, 2005). These MSE wall backfills were accepted based on AASHTO standards. The Association of Metallically Stabilized Earth (AMSE) offered a potential explanation for these consistently lower-than-predicted corrosion rates when it stated that the AASHTO specifications may have more than doubled the recommended galvanization thickness loss per year for use in corrosion models that was presented in the original research data (AMSE, 2006).

2.3 Underground (Soil) Corrosion

Corrosion of underground metal has been studied extensively by several Departments of Transportation (DOTs), federal agencies, and engineering organizations. Underground electrolytic corrosion studies of metal pipe were published as early as 1895 in *Transactions of the American Institute of Electrical Engineers* (Low, 1895). Stray current from electric rails was the main concern. Another major published study was the 45-year underground corrosion study of various metals and their coatings conducted by the U.S. Department of Commerce's National Bureau of Standards in its Circular 579 (Romanoff, 1957). Romanoff focused on the finer-grained soil electrochemical properties, which offered useful insight for future researchers in determining how grain size distribution, moisture content, temperature, electrical resistivity, and various other soil properties affect corrosion rates.

Corrpro Companies developed and verified methods to measure the laboratory and field corrosivities of soil based on estimated resistivities for buried pipe applications (Vilda, 2009). Elias (2000) of the Federal Highway Administration (FHWA) focused research efforts on applying Romanoff's data for galvanized steel to MSE wall reinforcement corrosion.

2.4 MSE Backfill Corrosivity

As MSE walls with galvanized steel reinforcement became popular post-1970, the corrosion research foundation laid by Romanoff and others acted as the basis for estimating MSE metal reinforcement corrosion. However, many researchers found that soil corrosivity characterization techniques for soil could not be effectively applied to aggregates. When subjected to leachate testing, different particle size ranges within a given aggregate exhibited different electrochemical properties (Thapalia, Borrock, Nazarian, & Garibay, 2011).

Castillo, Hinojos, Bronson, Nazarian, and Borrok (2014) proposed a method using an unsieved sample to address the particle size driven electrochemical property differences. This test essentially gave the average of the different electrochemical properties of the different particle sizes with one test on the liquid obtained from a leachate test. This method does address the findings from Thapalia et al. (2011) above, but still may not be representative of actual field conditions. The previous researchers, from Low (1895) to Castillo et al. (2014), have shown that electrical resistivity can effectively represent corrosivity, and so the challenge became how to accurately determine electrical resistivity of larger aggregates.

Edlebeck and Beske (2014) of the Institute of Electrical and Electronics Engineers (IEEE) developed a laboratory procedure to estimate the electrical resistivity of larger aggregates using electrical substation ground covering. This material is similar to MSE coarse aggregate backfill in both particle size and desired electrochemical property determinations. A known mass of unsieved material was first prepared to a specific moisture content and then was compacted into a known volume container (in this case, a 0.4 ft³ concrete block mold). The resistance of the material was measured using a Wenner 4-probe arrangement modeled from a combination of ASTM G57 and G187 (Edlebeck & Beske, 2014). This procedure controls major electrical resistivity influences such as moisture content and compaction.

2.5 Galvanized Steel Anatomy

According to the American Galvanizers Association (AGA), the galvanization process results in multiple layers of different steel-zinc alloys covered by a layer of pure zinc and underlain by the bare steel surface. These alloy layers adhere strongly to the steel and protect it

from corrosion for up to 75 years, depending upon environmental conditions. They consist of hard, abrasion-resistant material overlain by a soft, ductile layer of pure zinc, which provides impact resistance in addition to the abrasion resistance provided by the alloy layers. Since the steel is fully immersed in molten zinc, these layers provide 99 to 127 μm of corrosion barrier protection uniformly on every exposed surface (AGA, 2012).

2.6 Galvanized Steel Reinforcement Corrosion

As the freshly galvanized steel article is exposed to the air, oxidation of the top pure zinc layer begins, forming oxides of zinc. After the steel article is placed in the ground and is subject to enough wetting and drying cycles, a layer of strong, adhesive zinc carbonate (the dull grey zinc patina) forms. The new zinc carbonate layer is insoluble in water, which protects the remainder of the zinc layer from corrosion and reduces the corrosion rate of the newly patinated galvanized steel article to $\frac{1}{30}$ th that of bare steel in the same conditions. Depending on environmental conditions and the frequency of wetting and drying cycles, this patina takes anywhere from six months to a year to fully develop (AGA, 2012).

The zinc patina is the first of two stages in barrier protection to prevent corrosion of structural steel. The second stage in barrier protection is composed of the underlying steel-zinc alloy layers. As long as the bare steel remains unexposed to the outside environment, the abrasion resistant alloy layers provide the steel with a hard, adhesive layer of protection from the corrosive environment.

When the zinc patina and alloy layers are breached, cathodic protection becomes the primary means of preventing corrosion of the steel. During cathodic protection, the two-stage barrier protection provided by the zinc patina and its underlying alloy layers is compromised due to thinning. As these barriers thin, the steel becomes more and more directly electrically connected to the outside environment, increasing its own corrosion potential. The remaining zinc will act as the anode, the steel as the cathode, and the soil environment as the electrolyte in this bimetallic couple electrical circuit since zinc is more galvanically active than steel (iron). In a bimetallic couple, the anode is oxidized and the cathode is protected from oxidation. Since steel is forced to be cathodic by the presence of the zinc, steel is protected from corrosion, or

oxidation. This cathodic protection is effective even when the bare steel is exposed to the outside environment—so long as zinc is present within a certain diameter, the exposed steel will not begin to corrode (AGA, 2012).

Galvanization is advantageous over other corrosion protection methods due in large part to the three-stage protection system offered by the zinc with its two-stage barrier protection in addition to its cathodic protection. Also, since zinc is naturally occurring in most soils, its oxidation has no contamination potential.

2.7 Research Directions for MSE Backfill Corrosion Potential Characterization

Based on the literature, control of density for corrosion characterization of MSE coarse aggregate backfills in accordance with Edlebeck and Beske's (2014) methods for electrical substation ground cover should be considered. Corrosion studies are recommended to consider only galvanized steel reinforcement due to its advantages over other corrosion protection. Thapalia et al. (2011) recommend that samples for laboratory characterization not be sieved to a certain size due to the potential for different aggregate fractions to have different electrochemical properties. Yzenas (2014) has proposed such a procedure to ASTM International as ASTM C XXX-XX (hereafter referred to as the New ASTM) in which an unsieved aggregate sample is compacted into a two-electrode box, soaked in a specific type of water for 24 hours, drained, and then is tested to estimate electrical resistivity.

The following chapters illustrate differences between the New ASTM and the current method for electrical resistivity of aggregates and explore the New ASTM's applicability and repeatability.

Chapter 3: Research Scope

This chapter contains descriptions of the scope of work for this project, the materials used, and the tests performed on them. The standard AASHTO (2012) electrical resistivity test and the draft of a new ASTM aggregate resistivity test were both used except where noted. In addition to the research conducted at The University of Kansas (KU), Kansas State University (KSU) conducted field electrical resistivity tests on the same materials after their placement as backfill.

3.1 Materials Used

Five backfill samples were collected from four different retaining walls near the ends of their respective construction phases. This eased material collection and provided material as close to field conditions as could be achieved, but limited material collection to specific times. Sampling collection locations are reported in Table 3.1. All locations were in Kansas.

Table 3.1: Sample Collection Locations

| Material | Collection Location |
|---------------------------------|---|
| Colored I-70/K-7 | I-70/K-7 Interchange, SW Exit Ramp from I-70 to K-7, N of Bonner Springs |
| Gray I-70/K-7 | I-70/K-7 Interchange, SW Exit Ramp from I-70 to K-7, N of Bonner Springs |
| Pittsburg | Meadowbrook Mall, Pittsburg, NW Wall along Centennial Drive |
| Ridgeview | N Bridge Abutment on S Ridgeview Rd. crossing K10 W of Lenexa |
| South Lawrence Trafficway (SLT) | N Wall along new 31 st St. E of Haskell Intersection, Lawrence |

Sampling details are reported in Table 3.2. One wall under construction near Bonner Springs, Kansas, provided two visually different aggregate backfills; samples of both were collected. Material was manually collected in large trash cans in accordance with ASTM D75 (2014) unless noted otherwise. The sample size for each type of material was approximately 800 pounds (five 20-gallon trash cans, each approximately $\frac{2}{3}$ full). Trash can lids were taped shut on the way back from collection to prevent material contamination and loss.

Table 3.2: Sampling Details

| Material | Wall Length | Wall Max Height | Wall Type | Collection Source | Collect Date | Max Size | Color |
|---------------------------------|----------------------|--------------------|----------------------|--------------------|--------------|--|--------|
| Colored I-70/K-7 | 1,160 ft. (353 m) | 38 ft. (11.5 m) | Geogrid MSE | Stockpile ASTM D75 | 6/16/14 | 1" (25 mm) | Multi |
| Gray I-70/K-7 | 1,160 ft. (353 m) | 38 ft. (11.5 m) | Geogrid MSE | Compacted Backfill | 6/23/14 | 1" (25 mm) | Gray |
| Pittsburg | 380 ft. (116 m) | 7 ft. (2.1 m) | Geotextile MSE | Stockpile ASTM D75 | 7/25/14 | 1" (25 mm) | White |
| Ridgeview | 230 ft. (70 m) | 18 ft. (5.5 m) | Metal SINE-Strip MSE | Compacted Backfill | 9/19/14 | 3" (75 mm) | Orange |
| South Lawrence Trafficway (SLT) | 300 ft. (91 m) | 16 ft. (4.9 m) | Gravity MSE | Stockpile ASTM D75 | 2/24/15 | ³ / ₄ " (19 mm) | White |

A few notes about specific samples are as follows. The gray I-70/K-7 sample received light rain on top of the trash can lids on the way back from collection. The Pittsburg sample was collected from a stockpile using a front loader. The Ridgeview material visually had more fine particles than the other samples and originated from the Upper Farley ledge in the Sunflower Quarry near De Soto, Kansas.

3.2 Lab Tests

The tests used to characterize the five different materials are listed in Table 3.3.

Table 3.3: Material Tests

| Standard | Description |
|---------------------|----------------------------------|
| AASHTO T 27 (2014) | Sieve Analysis |
| AASHTO T 288 (2012) | Soil Electrical Resistivity |
| New ASTM | Aggregate Electrical Resistivity |

Additional information is provided in the following sections on the tests for which no standard procedure has been established, or for which the procedures for an existing test were modified for the purposes of this research.

3.2.1 AASHTO T 288 Soil Electrical Resistivity Test

AASHTO T 288 (2012) required 1,500 grams of material smaller than 2 mm in diameter (passing the No. 10 sieve). The material was soaked in water that had passed through a battery water deionizer (battery DI water) for at least 12 hours before being placed into the AASHTO box using finger pressure for compaction. The AASHTO box was 4.4 cm in inside height, 15.2 cm in inside length, and 9.8 cm in width between the two electrode plates (see Figure 3.1). After compaction and striking off the sample to the level of the top of the box, the filled AASHTO box was then connected to a resistivity meter that met the requirements of AASHTO T 288.

The resistance of the soaked material, its water content, and its wet mass were measured and the density of the material was calculated for correlation with its calculated resistivity. The measured material was then removed from the box, mixed with additional battery DI water, and recompacted into the box; the same measurements were taken and the process was repeated until the measured resistance reached a lower limit. Resistivity was then calculated by multiplying this minimum measured resistance by the cross-sectional area perpendicular to electron flow divided by the average distance between the two electrode plates. This geometric ratio is often called the box factor.

Figure 4.2 shows the AASHTO box filled with the first round of Pittsburg sample. Figure 3.2 shows the resistance measurement setup.

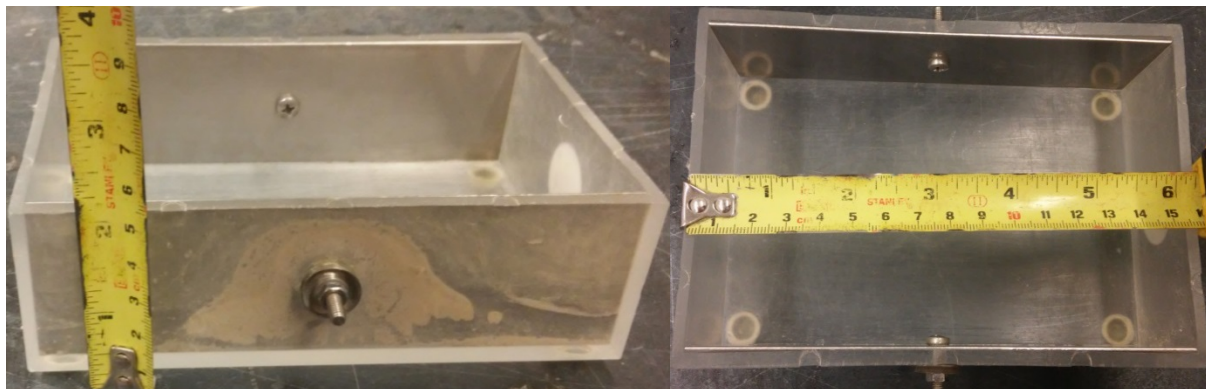


Figure 3.1: AASHTO Electrical Resistivity Box

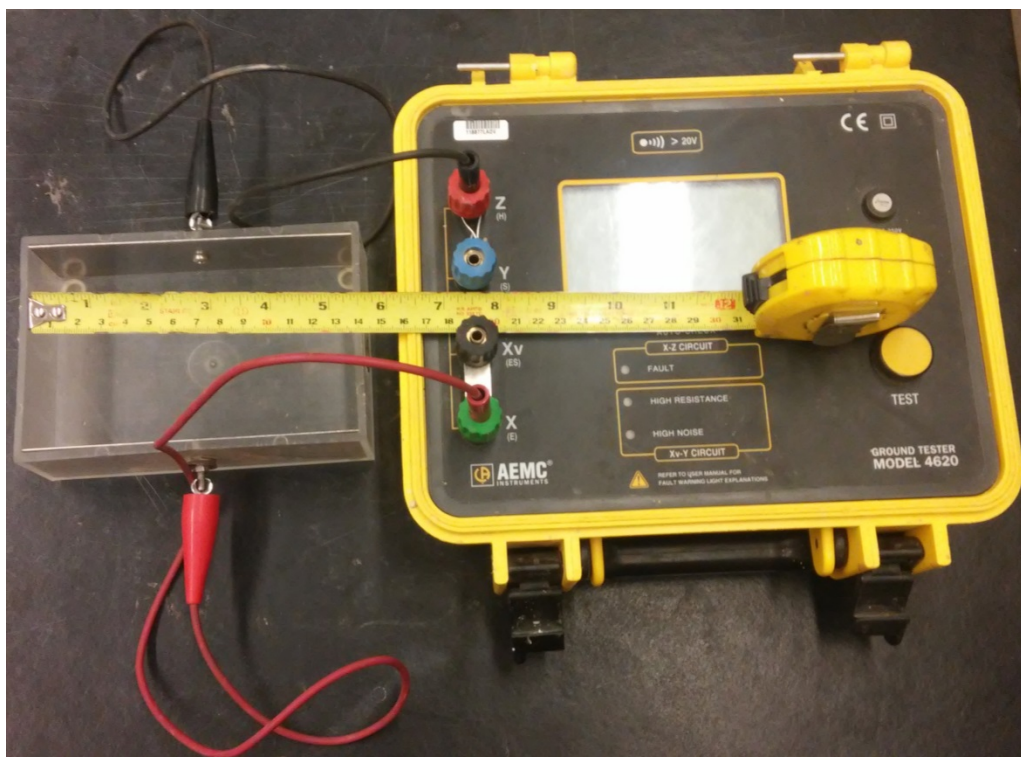


Figure 3.2: AASHTO T 288 Apparatus Setup

3.2.2 The New ASTM Aggregate Electrical Resistivity Test

The primary test used in this research was the most recent draft of a new ASTM aimed at obtaining the electrical resistivity of larger aggregates: ASTM C XXX-XX, *New Test Method for Measurement of Aggregate Resistivity Using the Two-Electrode Soil Box Method*. This New ASTM is a new procedure that has been proposed by John J. Yzenas Jr. for adoption by ASTM (Yzenas, 2014). This test procedure differs from AASHTO T 288 in several key ways for aggregate material. A summary of this test is presented in the following paragraph. Subsequent paragraphs describe the manipulation of different test parameters.

3.2.2.1 New ASTM Procedure

The amount of material required to run the New ASTM coarse aggregate resistivity test depended upon the size of the box used. The sample of material was first split to reduce the sample size to approximately match the amount required to fill the particular box; foreign material that should not have been in the sample (leaves, grass, dirt, etc.) was then removed. The

split sample was placed into the box in layers no deeper than 2 inches. Each layer was first wetted with the same battery DI water used in AASHTO T 288 (unless noted otherwise), and was then compacted by alternately lifting and then dropping each side of the box approximately 1 inch for 25 total drops per layer. After filling and then striking off the top of the material to approximately match the sample volume with the box inside volume, the same water type used to wet the aggregate layers was added into the box until full. The box was then left to soak for 23-25 hours under a covering to prevent contamination. During soaking, similar water was added as needed to maintain 100% saturation of the sample.

After soaking, the water in the Small, National Electrical Manufacturers Association (NEMA), and Large boxes was allowed to fully drain from the box via gravity, after which point the resistance of the resulting drained material was immediately measured. Full drainage for these boxes was assumed to have occurred when no more pore fluid was observed to drip out of the drain hole.

The ASTM and AASHTO boxes had no drain hole so as to preserve their manufactured form for other testing standards. After soaking, the water in these boxes was vacuum-drained using a wet/dry shop vacuum with $\frac{1}{8}$ -inch flexible tubing attached to the nozzle. Full drainage was assumed to have occurred when the level of water inside the box reached that of the bottom of the box.

To promote full drainage of the test material, all boxes were tilted toward their respective draining apparatus. This tilt was at first just below the friction angle of the material in the test box, but was reduced to approximately 10° to increase the stability of the box during draining. The different angles of drainage tilt appeared to have negligible effect on the results.

To calculate the resistivity of the material, the same procedure from AASHTO T 288 was used: measured resistance multiplied by geometric box factor equaled resistivity.

3.2.2.2 New ASTM Testing Parameter Variations

Throughout this research, soaking time, water type used, covering type, the number of soak/drain cycles, and the resistivity meter used during the New ASTM tests were all adjusted to determine their effects on the New ASTM resistivity test results.

Soaking times ranged from 5 hours to 80 hours. Water types used were either the battery DI water or tap water that had passed through a deionizer, an ultraviolet filter, and a reverse osmosis filter (RO UV DI). Rubber-banded plastic wrap was used for covering the boxes during soaking until it was observed that significant water was being removed from the box via the plastic's capillary action; rigid plastic plating was used for covering the boxes after this behavior was observed.

Several samples were soaked, permitted to drain, and soaked again in an attempt to simulate repeated infiltration cycles in the field. The first soak/drain cycled material (Cycle 1) was created using the same material sample as the original New ASTM test. After the initial resistivity measurement, the freshly drained material was soaked again for a number of hours (typically 24 to follow the new ASTM), drained, and then tested again, giving a result for once-drained material (Cycle 1). Cycle 2 material was created using the same procedure on the Cycle 1 material rather than the original New ASTM test sample.

For most tests the AEMC[®] Model 4620 ground resistivity meter was used, which meets the requirements of AASHTO T 288 and costs approximately \$2,000. This AEMC meter has a maximum display limit of 2,000 ohm, which is too small for the material used in boxes with smaller geometric box factors, such as the AASHTO box and especially the Miller box. This limit corresponds to a sufficiently high resistivity for most boxes so it should not be a problem in practice for pass/fail type testing using the current resistivity standard, but for the purposes of this research and correlation with other material properties, determination of the actual resistivity value was necessary. To address this equipment limitation, the resistivity meter used for KSU's field tests was also used for a few of the Gray I-70/K-7 material resistivity tests. This meter, a SuperSting R8 IP Earth Resistivity Meter (SSR8), cost over \$30,000 but offered a much higher maximum display limit of at least 60,000 ohm, which allowed comparison of ASTM and AASHTO box results with the results for the other boxes.

3.2.2.3 New ASTM Test Boxes

Samples were tested in five different boxes, the dimensions of which are shown in Table 3.4. Pictures of the boxes are shown in Figure 3.1 (AASHTO box) and Figures 3.3 through 3.5.

Table 3.4: Electrical Resistivity Box Details

| Box Name/ Identification | Height (cm) | Length (cm) | Electrode Separation (cm) | Box Volume (cm ³) | Electrode Area/L Factor (cm) | Box X-Section Area/L (USED) Factor (cm) |
|-----------------------------|----------------|----------------|---------------------------------|-------------------------------------|---------------------------------------|--|
| AASHTO | 4.4 | 15.2 | 9.8 | 654 | 6.8 | 6.8 |
| Small | 15.0 | 23.9 | 7.0 | 2,510 | 51.2 | 51.2 |
| NEMA | 14.5 | 34.9 | 24.0 | 12,145 | 21.1 | 21.1 |
| Large | 19.8 | 45.3 | 14.9 | 13,320 | 60.4 | 60.4 |
| Miller | 3.3 | 3.9 | 19.9 | 241 | 0.47 | 0.61 |

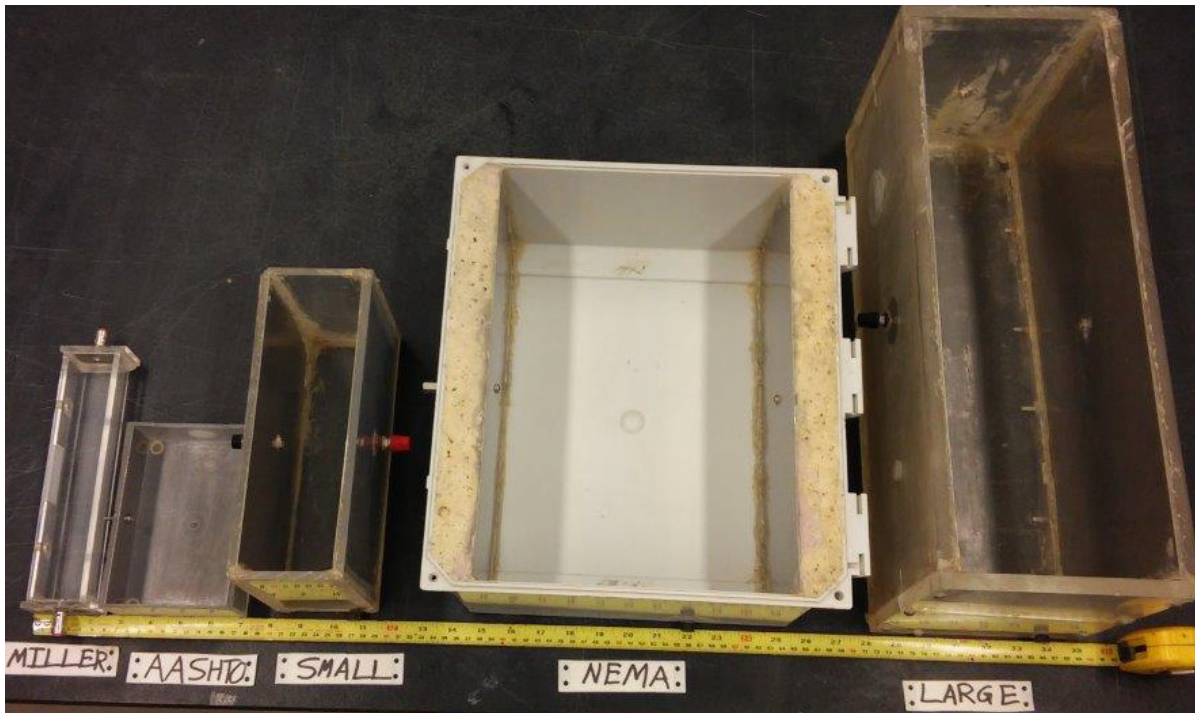


Figure 3.3: New ASTM Test Boxes Measured Perpendicular to Electrode Plates (Top View)

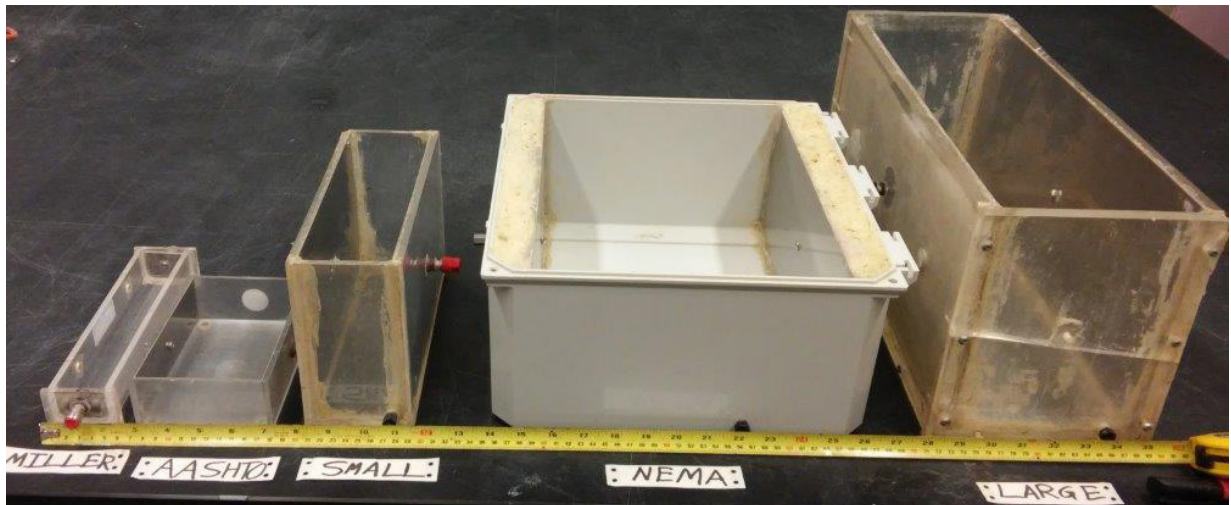


Figure 3.4: New ASTM Test Boxes Measured Perpendicular to Electrode Plates (Oblique View)

The Small and Large boxes were constructed using polycarbonate sheet connected at right angles edge to edge and sealed with silicone sealant to prevent liquid loss during soaking. The NEMA box started as a commercial polycarbonate electrical box. Stainless steel electrode plates and the drain plug were installed by KU. The Small, NEMA, and Large boxes each had a drain hole closed by a threaded, plastic drain plug of 9.5-mm outside thread diameter installed to allow water in the box to drain fully. Figure 3.5 shows the NEMA box with its drain plug. The AASHTO and Miller boxes were purchased from manufacturers and were certified to meet the AASHTO and ASTM standards for resistivity, respectively.



Figure 3.5: NEMA Box Outside (left) and Inside (right) with Threaded Drain Plug

All boxes were constructed using polycarbonate sheeting thick enough to be rigid during the compaction procedure. The electrode plates in the AASHTO, Small, NEMA, and Large boxes were all fabricated from stainless steel sheet metal and were cut to exactly match the inside dimensions of the electrode sides of each box. The Miller box electrode plates were installed by the manufacturer and covered approximately 77% of the curving cross-sectional area of the electrode sides of the box. Gaps behind the electrode plates installed in the Small, NEMA, and Large boxes were filled with nonconductive, expansive foam where practical and then sealed with silicone to prevent liquid inflow.

The Miller and Large boxes were both initially constructed for 4-probe measurements, but were converted to 2-probe configurations both to follow the New ASTM procedure and to maximize the box factor to maximize the usage of the AEMC meter 2,000-ohm maximum display limit. For all New ASTM tests, the box factors used for calculation are shown in the last column of Table 3.4 (box cross-sectional area divided by average electrode spacing).

Chapter 4: Test Results and Discussion

Figure 4.1 shows the grain size distribution of all five samples tested in this research. Note the Ridgeview and South Lawrence Trafficway (SLT) distributions near the 1-mm diameter. As shown later, these two samples exhibited the lowest resistivity values for the New ASTM test.

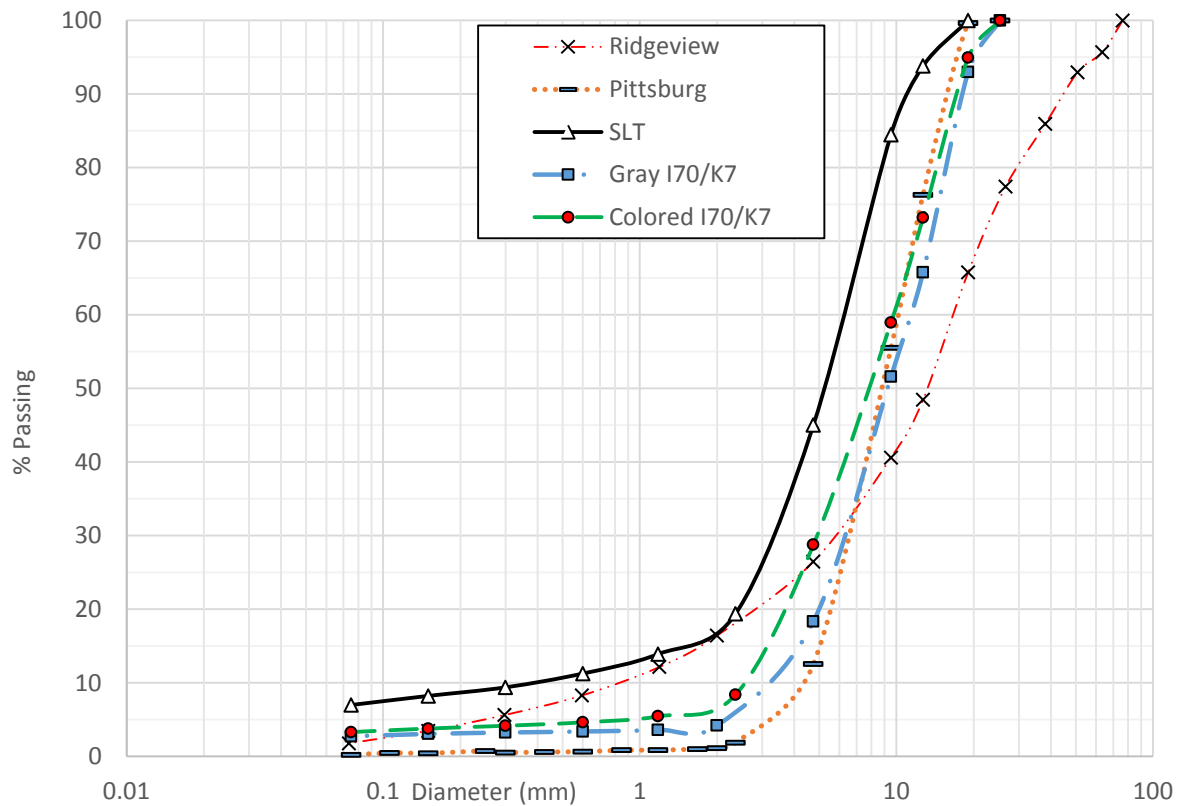


Figure 4.1: Grain Size Distributions of Samples from MSE walls

4.1 AASHTO T 288 Electrical Resistivity

4.1.1 AASHTO T 288 Pittsburg Results

The AASHTO T 288 (2012) test was conducted with approximately 1,500 g of dry Pittsburg material passing the No. 10 (2-mm) sieve. The minimum resistivity of 6.48 ohm-m

occurred at a moisture content of 128%. The mass of solids compacted into the box in the first round was 1,223 g; this number was 416 g by the 11th round, at which the minimum resistance was measured. This represented a 66% mass loss of material to obtain the minimum resistivity. Figure 4.2 shows the filled box during the first round. The moisture content is approximately 10%.



Figure 4.2: Filled AASHTO Resistivity Box (Pittsburg, minus No. 10, w = 10 %)

Figure 4.3 shows the moisture content samples for each of the 13 rounds conducted. The moisture contents increase with each round, so the rounds progress in the figure starting from the top and spiraling clockwise inward until reaching the 13th round, represented by the leftmost smaller container. The wet samples filled the containers to the brim; the right picture is tilted to visualize the amount of moisture loss during drying.



Figure 4.3: Moisture Samples for Each Pittsburg Round (Left: Wet; Right: Dry)

Table 4.1 shows moisture content and resistivity of the Pittsburg material used for each round.

Table 4.1: AASHTO T 288 Results (Pittsburg)

| Trial | Resistivity (Ohm-m) | MC % |
|------------|---------------------|--------------|
| R1 | 67.51 | 9.8 |
| R2 | 20.46 | 15.6 |
| R3 | 16.07 | 21.6 |
| R4 | 13.17 | 26.5 |
| R5 | 12.09 | 31.0 |
| R6 | 9.99 | 55.1 |
| R7 | 8.84 | 58.3 |
| R8 | 7.43 | 112.6 |
| R9 | 7.09 | 88.0 |
| R10 | 6.89 | 105.5 |
| R11 | 6.48 | 127.9 |
| R12 | 6.55 | 137.8 |
| R13 | 6.68 | 152.1 |

The minimum resistivity reported for the Pittsburgh material according to AASHTO T 288 occurred in R11, 6.48 ohm-m. R8's moisture content discrepancy may be attributed to an unrepresentative sample because it was difficult to equally collect all representative parts of the resulting slurry. Linear interpolations with respect to both the mass of solids in the box compared with those of R7 and R9 and the resistivity compared with those of R7 and R9 yielded moisture contents of 83.6% and 82.2%, respectively. It is thus reasonable to assume that the actual moisture content of R8's material was approximately 83%, and not 113%.

4.1.2 AASHTO T 288 Ridgeview Results

AASHTO T 288 was conducted with approximately 1,500 g of dry Ridgeview material passing the No. 10 (2-mm) sieve. The minimum resistivity of 6.62 ohm-m occurred at a moisture content of 280%. The mass of solids compacted into the box in the first round was 1,013 g; this number was 217 g by the 12th round, at which point the minimum resistance was measured. This represented a 79% mass loss of material to obtain the minimum resistivity. Figure 4.4 shows the moisture content samples for each of the 13 rounds conducted. The moisture contents increase with each round, so the rounds progress in the figure starting from the top left and progressing to the right for each subsequent row, similar to reading an English book. The wet samples filled the containers to the brim; the right picture is tilted to visualize the amount of moisture loss during drying. Table 4.2 shows moisture content and resistivity of the Ridgeview material used for each round.

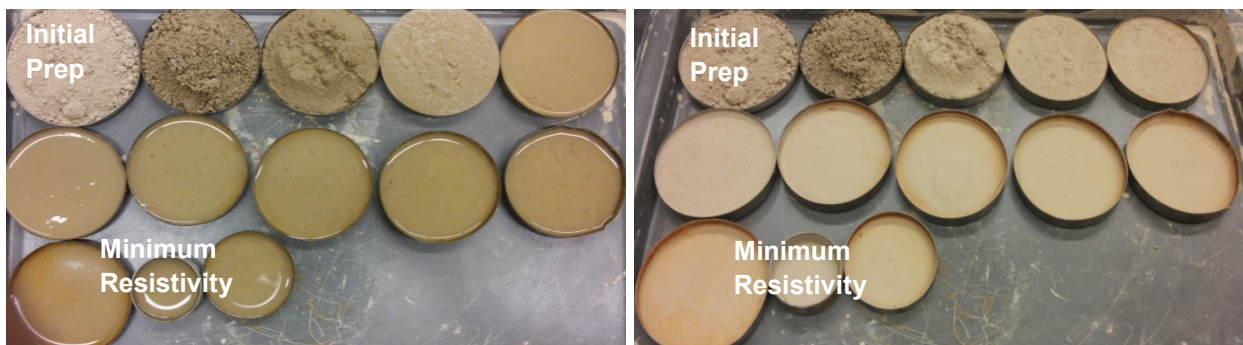


Figure 4.4: Moisture Samples for Each Ridgeview Round (Left: Wet; Right: Dry)

Table 4.2: AASHTO T 288 Results (Ridgeview)

| Trial | Resistivity (Ohm-m) | MC % |
|--------------|--------------------------------|-------------|
| R1 | >135 | 1.02 |
| R2 | 48.6 | 9.16 |
| R3 | 20.2 | 16.2 |
| R4 | 17.4 | 22.0 |
| R5 | 13.6 | 30.6 |
| R6 | 11.7 | 39.3 |
| R7 | 8.78 | 99.0 |
| R8 | 7.68 | 73.6 |
| R9 | 6.84 | 163 |
| R10 | 6.84 | 210 |
| R11 | 6.74 | 279 |
| R12 | 6.62 | 280 |
| R13 | 7.24 | 400 |

4.1.3 AASHTO T 288 Discussion

According to AASHTO T 288, the Pittsburg material failed to meet the minimum resistivity requirement of 50 ohm-m. Considering the moisture content of the round of interest was over 100%, this 6.48 ohm-m value is unlikely to be representative of field conditions. To represent field conditions, there would have to be in the field a highly segregated (minus 2 mm) pocket of essentially undrainable material in contact with a significant portion of the metal reinforcement. This is unlikely since MSE walls are required to be constructed using free draining and well-mixed backfill material.

Obtaining enough Pittsburg material for AASHTO T 288 required sieving approximately 68 kg (150 lb) of original sample because the fraction of material smaller than 2 mm in diameter was so low. It is possible that the minus-2-mm material had different mineralogy than the larger material rejected from the test sample. Not only was a great deal of sieving required to obtain enough acceptable sample for this test, but the mineralogies of the material passing the No. 10 sieve (2 mm) and the material retained on the No. 10 sieve may have been quite different (shale

and limestone). Since limestone is typically more durable than shale, and shale is often found interwoven through the bedrock layers blasted and crushed in the quarry for MSE backfill material, the shale content of any MSE backfill sample is likely overrepresented in the particle size range accepted for this test. Additionally, visual observation of all minus-2-mm material revealed an orange tint regardless of the color of the larger aggregate from the same source material. Thus, testing only the aggregate fraction passing the No. 10 sieve for electrical resistivity testing may bias the sample composition toward weaker materials more prone to breakage and pulverization. Therefore, the tested material may not be representative of the target material.

The resistivity of the Ridgeview material was also reported using AASHTO T 288 by Snapp (2015) as 60 ohm-m. This result is much higher than the resistivity of the same material reported as 6.6 ohm-m in this research. This discrepancy is likely due to a difference in procedure and possibly a material difference in samples. The values reported by Snapp were likely generated using a modified version of the T 288 test which calls for adding water up to and not beyond 100% saturation, rather than adding water until a minimum resistivity was obtained (which most often resulted in supersaturation and exclusion of a portion of the solids from the tested sample) as specified in T 288 and as was done for this project.

4.2 New ASTM Results

Since AASHTO T 288 may provide resistivity results based on conditions considered unrepresentative of field conditions, the New ASTM test procedure was tested extensively for its repeatability and field applicability to properly designed and constructed MSE walls.

A total of 69 New ASTM tests were conducted. Often, the box factors of the smaller, commercially available boxes (AASHTO and ASTM) caused resistance readings to exceed the maximum limit of the AEMC meter; therefore, results for these tests could not be obtained. This condition represented almost $\frac{1}{4}$ of the total number of New ASTM tests conducted, and reflects an issue that is likely to occur often if the ASTM test is used. Because the resistivity was typically significantly higher when measured with this test compared with the AASHTO test, use of the traditional small boxes with small box factors often resulted in resistance values that were

too high to be measured with a standard 2,000 ohm ground resistivity meter. For the AEMC meter used, zero of seven New ASTM tests conducted in the Miller box yielded calculable resistivity results. This problem can be solved by using a box with a sufficiently large box factor.

Figure 4.5a shows New ASTM results as a function of box factor. Figures 4.5b through 4.5d show the results as a function of box cross-sectional area perpendicular to electron flow, box volume, and box electrode spacing, respectively. Figure 4.5e shows proposed trendlines based on the data from Figure 4.5d. ‘Normal’ data points represent tests that followed the New ASTM, i.e. 24 +/-1 hour soaking time of original sample material, in addition to use of the AEMC meter and battery DI. Deviations from this procedure are noted in the legends and trendlines for each figure where applicable. The maximum calculable resistivity possible in the AASHTO box was 135 ohm-m (2,000 ohm resistance reading high limit multiplied by the 0.0675-m box factor), denoted by the blue line near each AASHTO labeled data set. Similarly, the maximum calculable resistivity for material in the Miller box was 12 ohm-m, which is much lower than the required 50 ohm-m KDOT lower limit for MSE backfill.

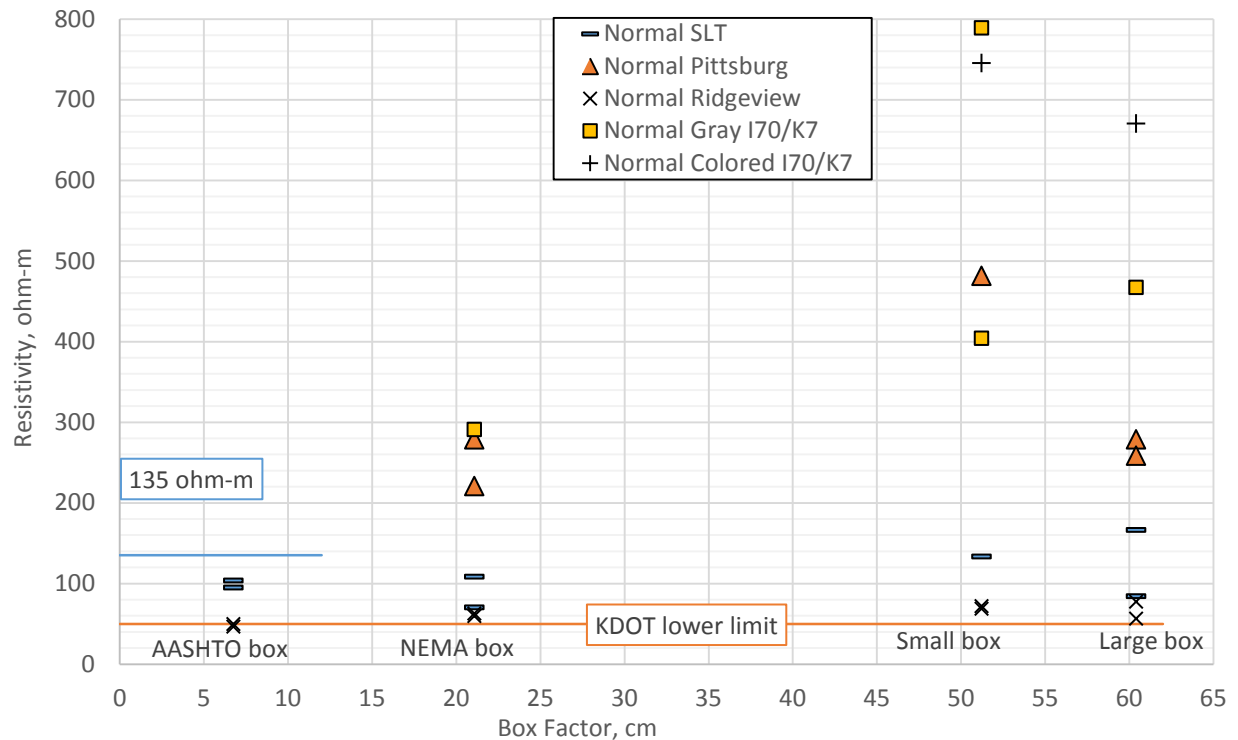


Figure 4.5a: All New ASTM Normal Results vs. Box Factor

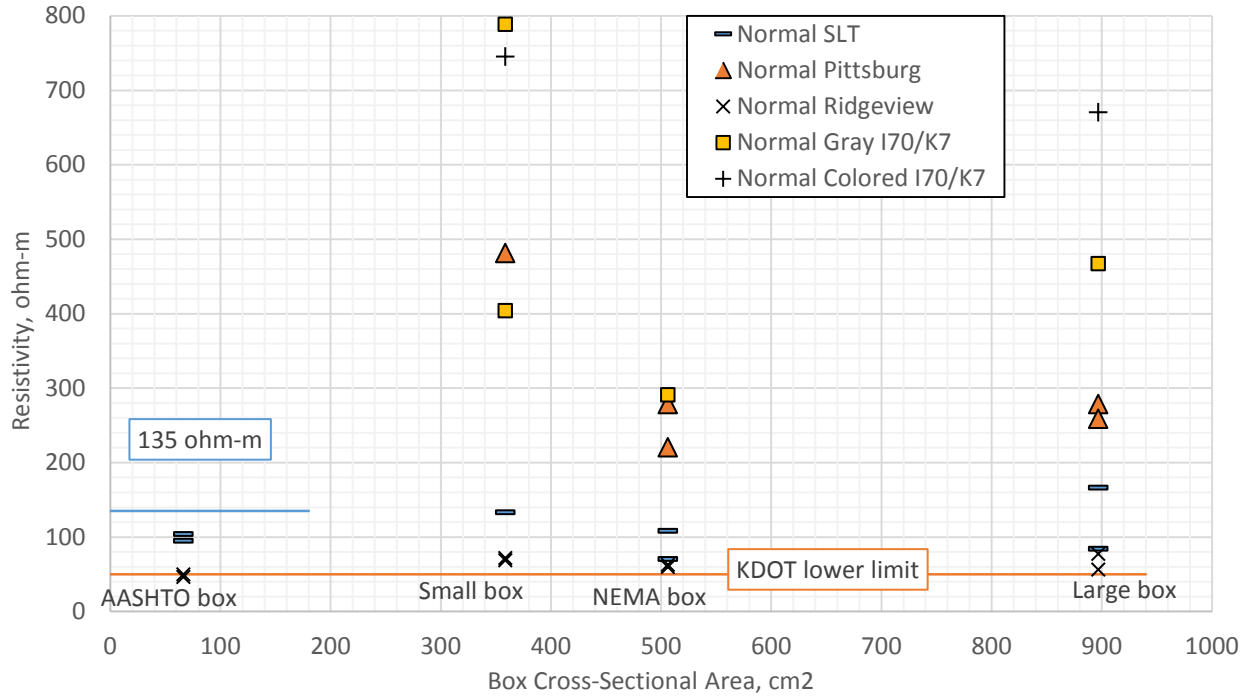


Figure 4.5b: All New ASTM Normal Results vs. Box Cross-Sectional Area Perpendicular to Electron Flow

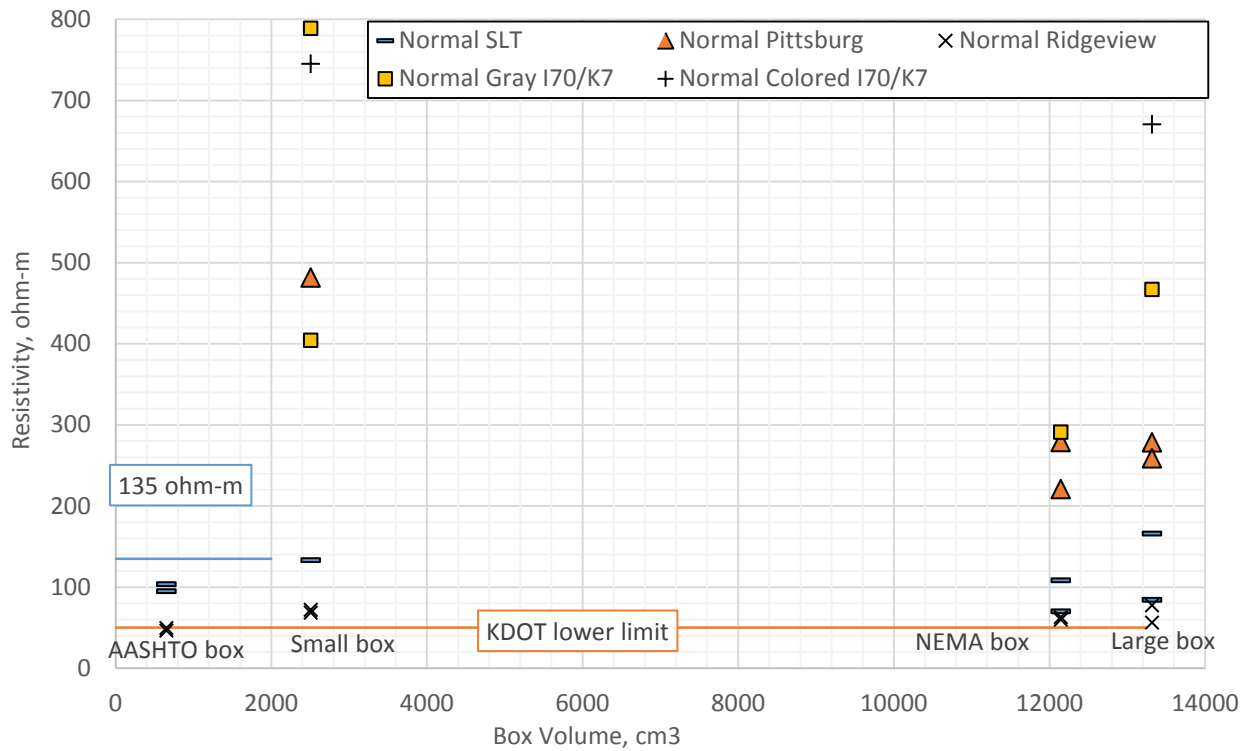


Figure 4.5c: All New ASTM Normal Results vs. Box Volume

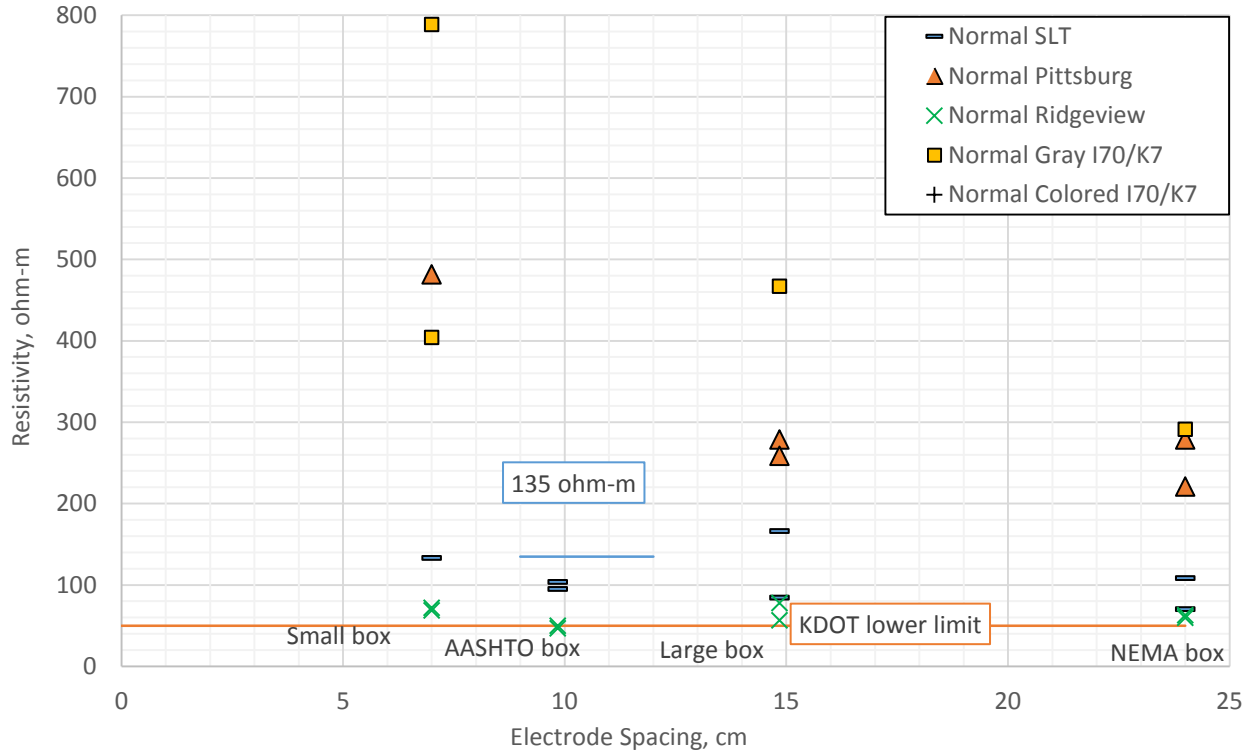


Figure 4.5d: All New ASTM Normal Results vs. Electrode Spacing

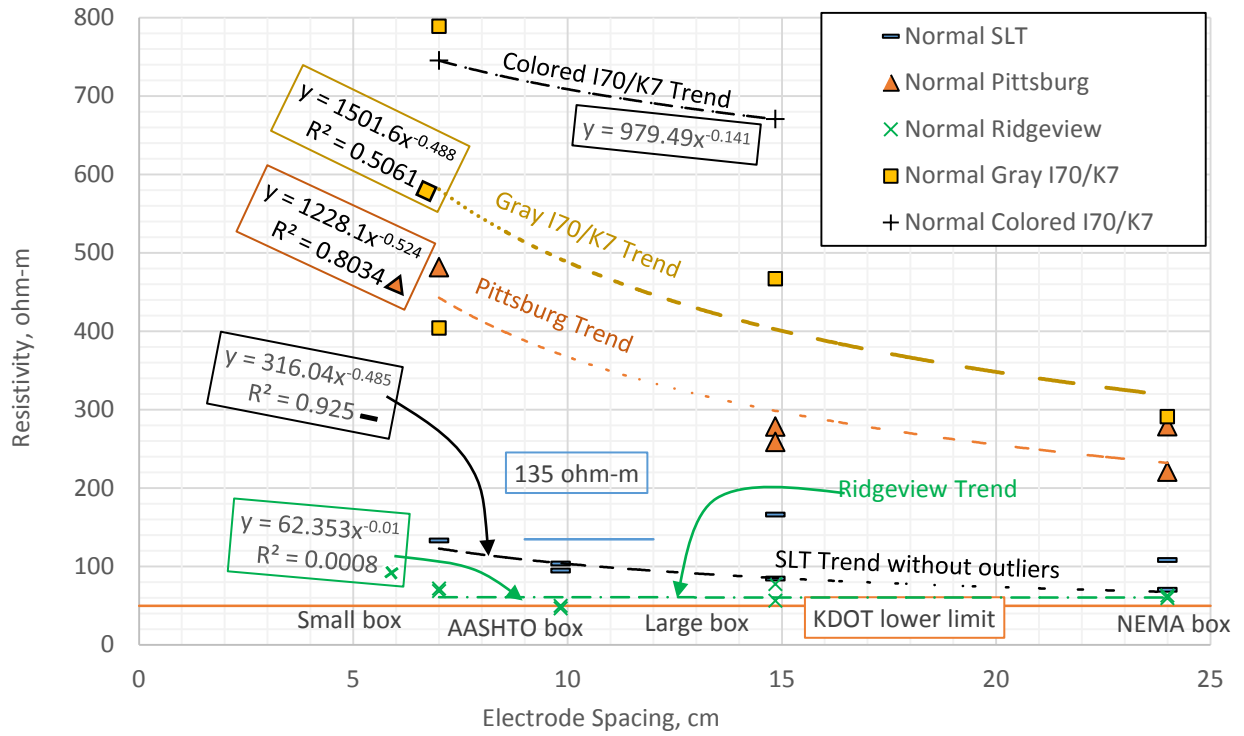


Figure 4.5e: All New ASTM Normal Results vs. Electrode Spacing Trends

Electrode spacing seemed to offer the best correlation, and thus was chosen for display of material-specific results below. The KDOT minimum resistivity of 50 ohm-m is plotted on each of these figures. In addition, the KSU field bulk electrical resistivity (ER) data labeled “Snapp Bulk ER, [value in ohm-m]” are included for comparison. Figure 4.5e displays trendlines of note based on data from Figure 4.5d. Additional resistivity results with resistivity plotted versus geometric parameters other than box factor are presented in Appendix A.

Snapp reported both dry and wet bulk ERs for select walls. Where possible, the wet bulk ER was used for comparison with the results obtained in this research for each material due to similar moisture conditions resulting from recently wetted and then gravity drained material. Care must be taken when comparing results from a particular laboratory box to the bulk ER, as the potential exists for there to be variations in moisture content, compaction, mineralogy, and other material properties between the box sample and the bulk ER tested compacted backfill.

It appears from Figure 4.5e that as the electrode spacing increased, both the spread of the resistivity results and their average values decreased. This was most likely due to the larger distance between the electrical pulse origin and destination, which tended to reduce the exaggerated effects of larger particle sizes on the electrical flow path length. In other words, the larger the ratio of electrode spacing to maximum particle diameter, the fewer electrical flow path distance outliers there will be because the greater distance between electrodes will tend to “average out” the effect of very large particles on the electrical flow path.

It appears that the majority of single material resistivity values in ohm-m exhibited an approximate power law relationship of exponent -0.5 with electrode spacing in cm. The colored I-70/K-7 material may not have been tested enough to verify this power law. The SLT ‘outliers’ are discussed further in Section 4.2.1 and the Ridgeview data is discussed further in Section 4.2.3.

4.2.1 SLT Material New ASTM Resistivity Results

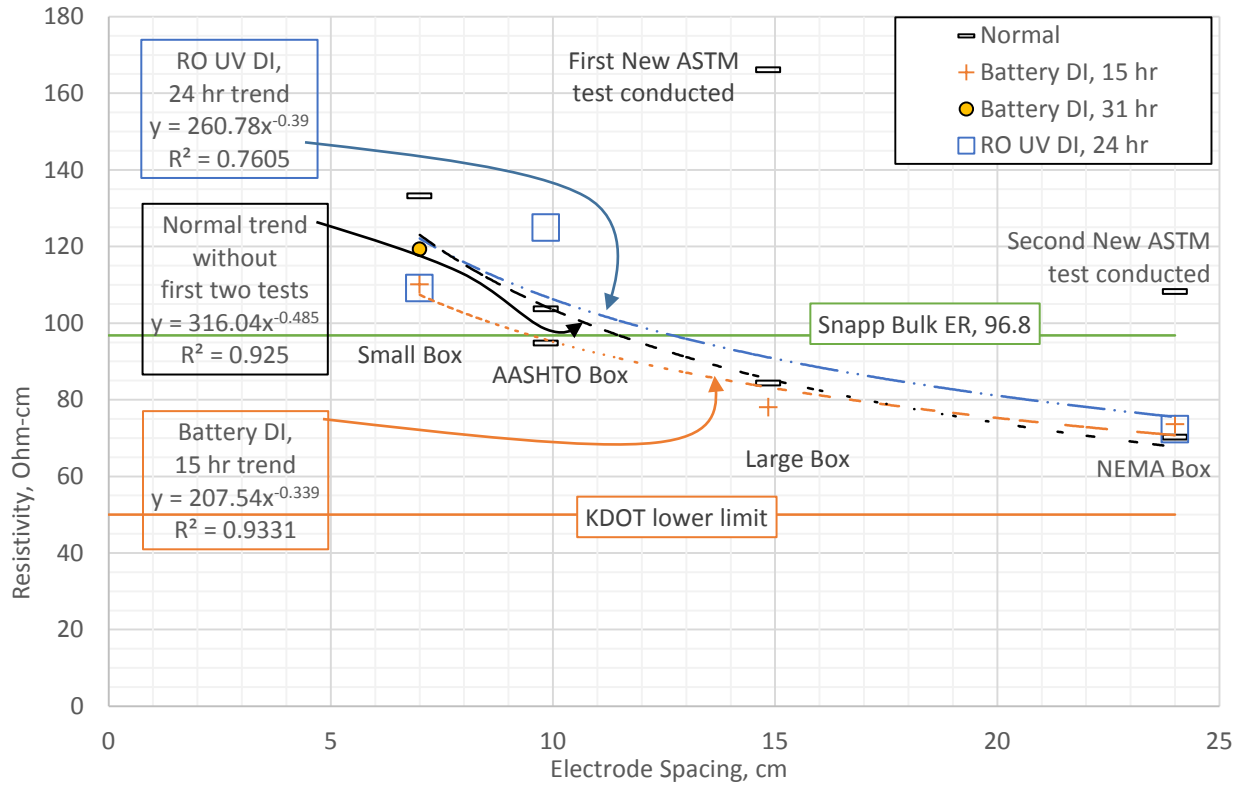


Figure 4.6: SLT New ASTM Results vs. Electrode Spacing

Figure 4.6 shows the resistivity of the SLT material as a function of electrode spacing. The SLT results generally follow the trend of Figure 4.5e with both the calculated resistivity spread decreasing and values decreasing as electrode spacing increased, with the exceptions of the Large box result over 160 ohm-m and the NEMA result over 100 ohm-m. These were the first two New ASTM tests conducted for this project. This discrepancy may be due to differing compaction degrees as the testing style and procedure was still being adjusted to accommodate the specific laboratory conditions and equipment. These tests were repeated, and results similar to those for the battery DI test for the Large box and the battery DI test for the NEMA box were obtained. Considering that the two initial tests may have differed slightly from the others as the procedure, especially regarding compaction, became routine, the NEMA box appears to have given the lowest and most accurate values of material resistivity regardless of the soaking time

and the water type used. Please note the y-scale differences between Figures 4.5e and 4.6. The decline in resistivity with electrode spacing appeared to taper off for an electrode spacing above 20-25 cm (8-10 inches). This is approximately 12 times the maximum particle size for this aggregate.

The Normal tests seem to follow the proposed trendline well if the first two New ASTM tests conducted were ignored. The other tests also fall within the same range, which suggests that the various adjustments to the New ASTM procedure represented by those other data points have limited or negligible effect on the calculated resistivity.

KSU bulk resistivity field test data for the wet condition is also plotted in Figure 4.6. As shown in the figure, this field resistivity data was very consistent with the lab New ASTM data.

4.2.2 Pittsburg Material New ASTM Resistivity Results

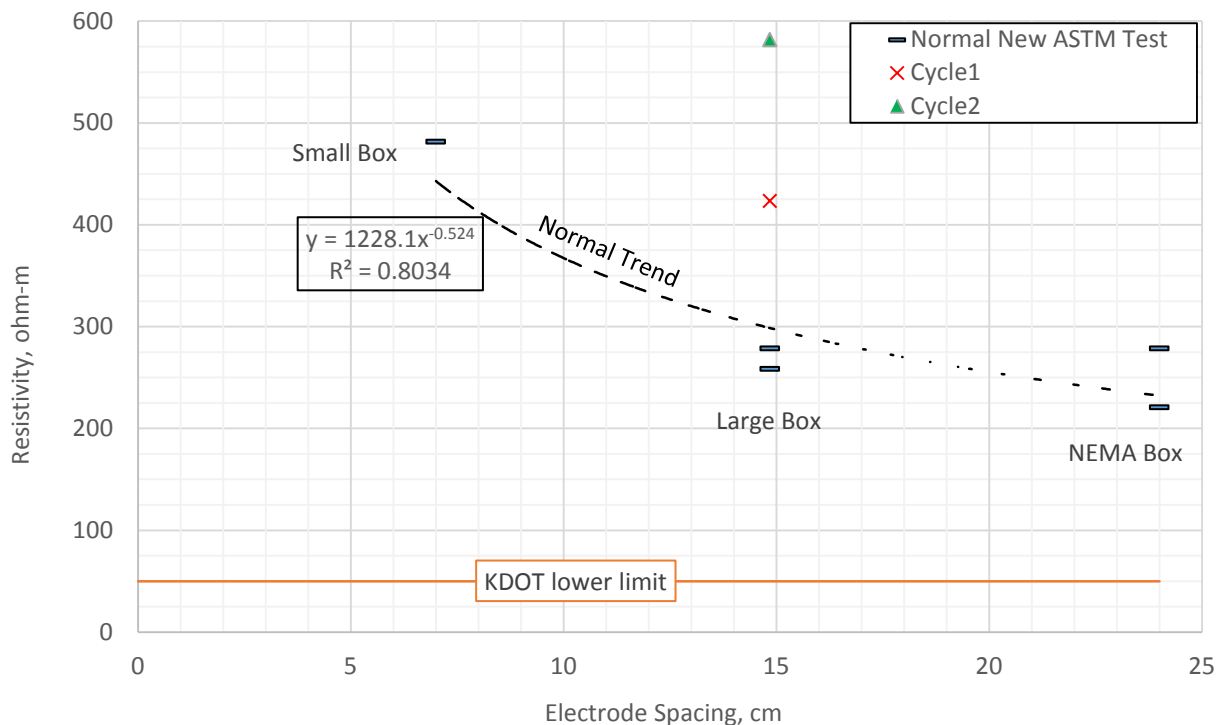


Figure 4.7: Pittsburg New ASTM Results vs. Electrode Spacing

Figure 4.7 shows the resistivity of the Pittsburg material as a function of electrode spacing. As with the SLT material, the Pittsburg material seemed to follow the general trendline set by Figure 4.5e with the NEMA box samples having the lowest resistivity. For this test, the Large box gave the most precise Normal results, represented by the 14.9 cm electrode spacing data. The two higher results (red X and green Δ) represent once- and twice-drained material, which are different materials than the original Pittsburg material as each soak/drain cycle removed a significant percentage of finer particles from the original sample. Overall, the NEMA box still appears to give the most conservative results. Please take note of the y-scale differences between Figures 4.5e and 4.7. The decline in resistivity with electrode spacing appeared to taper off for an electrode spacing greater than 15-20 cm (6-8 inches). This is approximately 7 times the maximum particle size for this aggregate.

4.2.3 Ridgeview Material New ASTM Resistivity Results

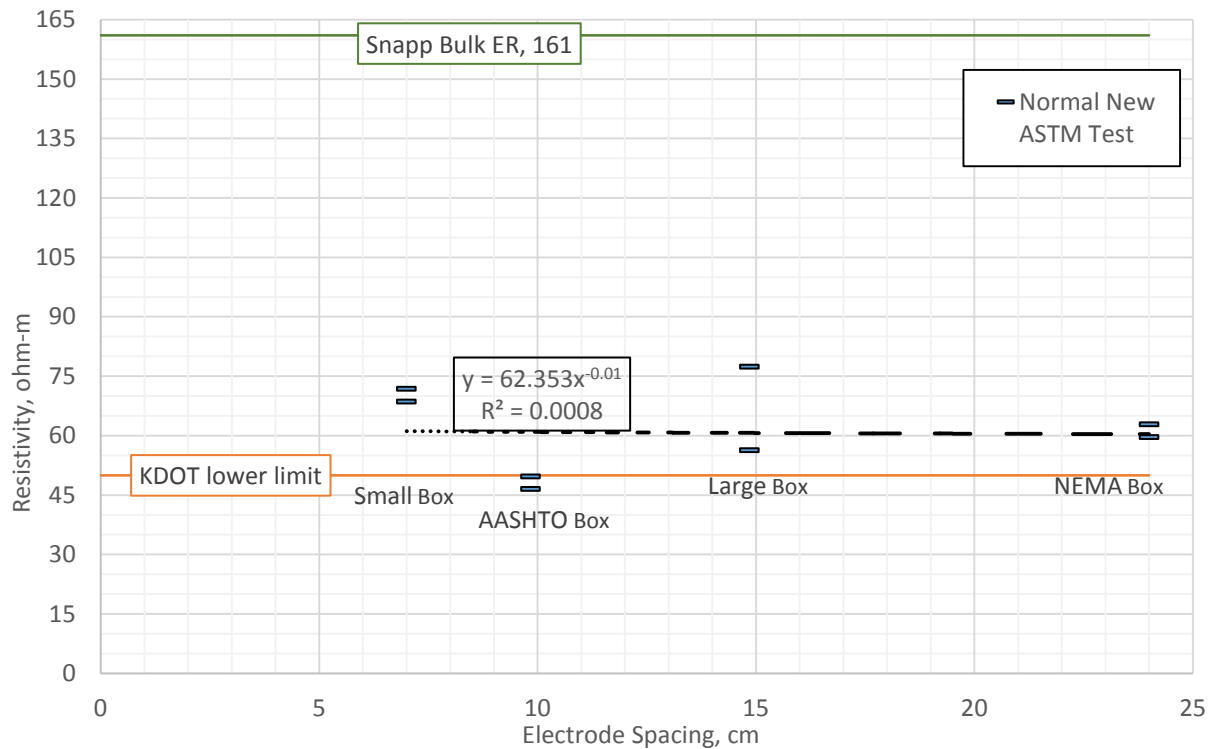


Figure 4.8: Ridgeview New ASTM Results vs. Electrode Spacing

Figure 4.8 shows the resistivity of the Ridgeview material as a function of electrode spacing. The Ridgeview results show that neither AASHTO box sample complied with KDOT specifications for electrical resistivity based on T 288 testing only, and additional testing (sulfates using AASHTO T 290 and chlorides using AASHTO T 291) would be required to fully characterize the Ridgeview material prior to acceptance for use. This particular material failed to drain when the plugs on any of the boxes were removed. This failure to drain was not seen in any other material, which may explain why this Ridgeview data power law fit has such a low R^2 value (essentially zero) compared with the other material data fit curves. The R^2 value indicates that electrode spacing of the test box has virtually no effect on the resistivity of the Ridgeview material.

In order to obtain the drained readings, a small metal rod was inserted into the open drain hole. After a flow path through the thick layer of finer material blocking the drain was opened, the water level decreased until it reached the finer material layer, at which point drainage slowed to essentially zero. This particle size segregation and drain blocking was seen in all Ridgeview samples tested, and may explain why the Ridgeview material resistivity results were as much as one order of magnitude lower than the results for the other materials. Please take note of the y-scale differences between Figures 4.5e and 4.8. Figure 4.9 shows selected boxes with this ‘Ridgeview effect.’ This may explain why the Ridgeview material did not seem to follow any discernible trend. The Snapp Bulk ER for wet Ridgeview backfill was also much higher than the lab results due most likely to the drainage issue.

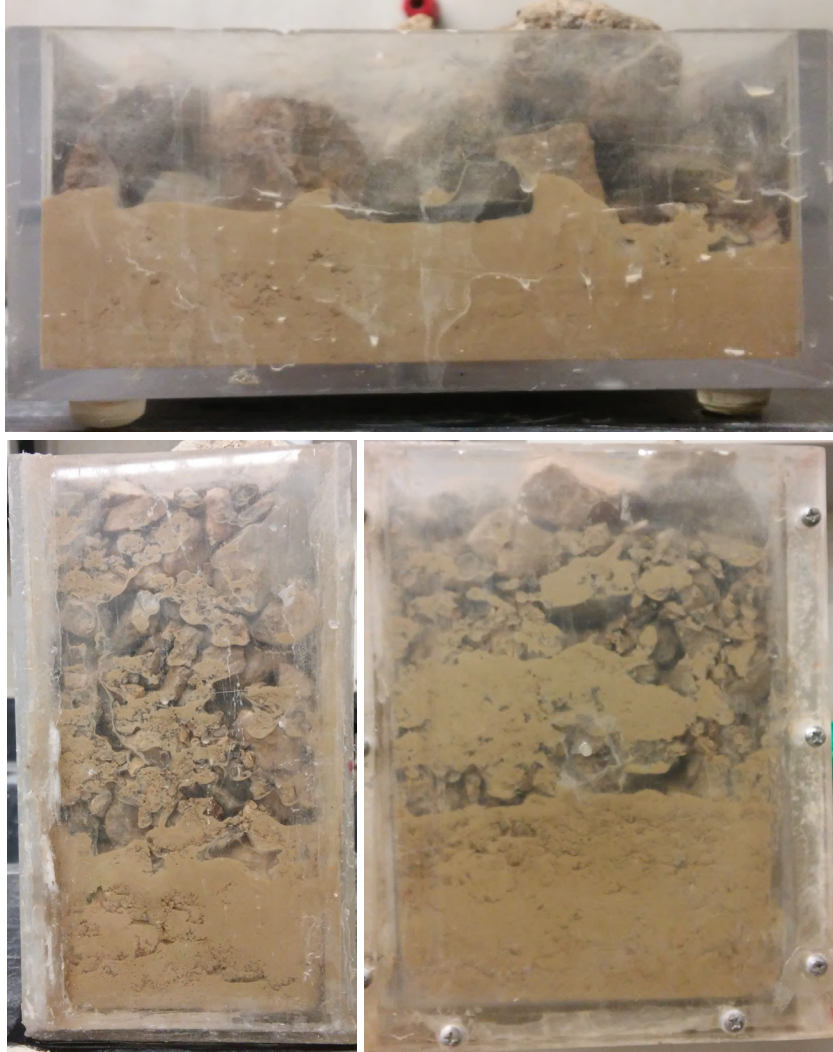


Figure 4.9: Ridgeview New ASTM Samples After Soaking and Attempted Draining; AASHTO box (top), Small box (left), and Large box (right)

4.2.4 Gray I-70/K-7 New ASTM Resistivity Results SSR8 meter

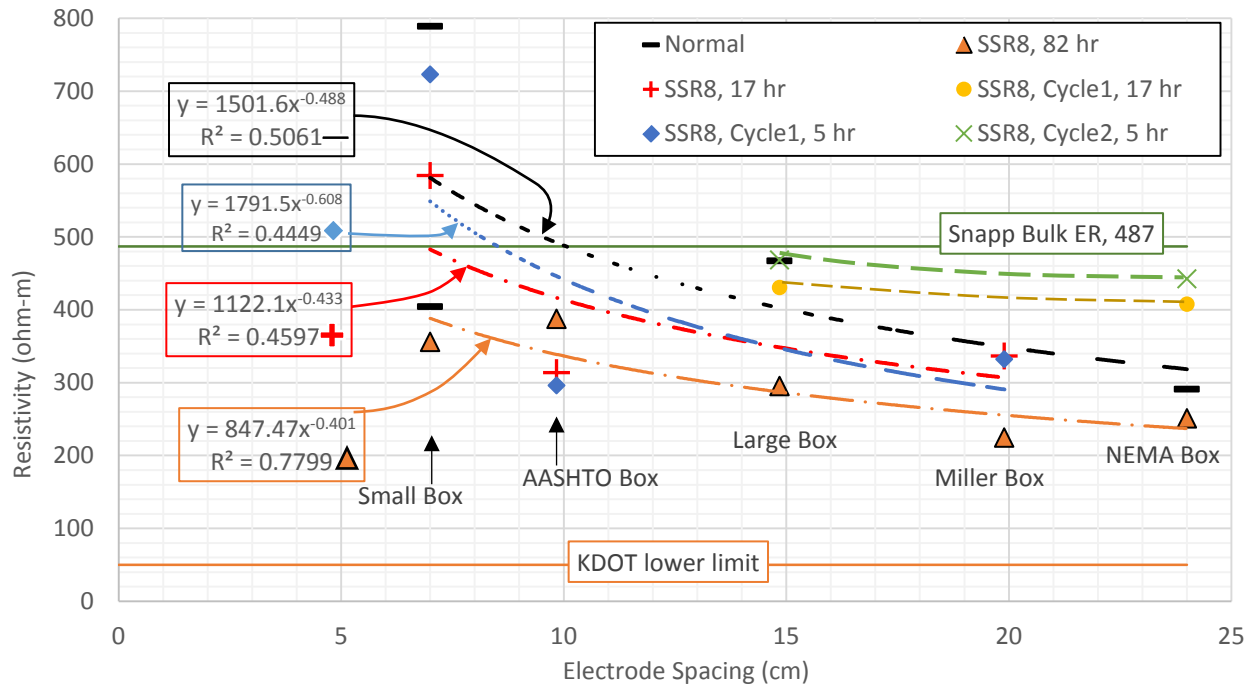


Figure 4.10: Gray I-70/K-7 New ASTM Results vs. Electrode Spacing

Figure 4.10 shows the resistivity of the Gray I-70/K-7 material as a function of electrode spacing. The Gray I-70/K-7 results also generally follow the trend of Figure 4.5e, although with more scatter than previously discussed aggregates. There was a particularly large amount of scatter in the Small box, which had the smallest electrode spacing. The SSR8 resistance values for this aggregate were measured using the SuperSting R8 (SSR8) meter. The Miller box gave similar and relatively precise results compared with the other boxes, most notably the NEMA box, which had been the best thus far. This was not expected due to the small size of the samples for this box, which should have reduced test repeatability. For this material, the Miller box appeared to give the most conservative result for the Gray I-70/K-7 material.

The trendlines also show that calculated resistivity generally decreased with increased electrode spacing regardless of soaking time, type of meter used, or number of soak/drain cycles. The samples soaked for 82 hours prior to draining appeared to have generally lower calculated

resistivities than the samples soaked for either 5 or 24 hours. The Snapp Bulk ER for dry I-70/K-7 material was consistent with the lab data.

Most trendlines in Figure 4.10 exhibit an approximate power law pattern with an exponent of -0.5. This suggests that electrical resistivity is a function of electrode spacing in the boxes, with a different soaking time changing the multiplying constant of the power law to intercept the y-axis at different values. Cycled tests also mostly resulted in higher resistivities. The 5-hour soaked Cycle 1 material may not have soaked long enough for direct comparison to the Normal tests regarding the effect of increased soak/drain cycles. The resistivity decline with electrode spacing flattened out for most test procedures at a ratio of electrode spacing to maximum aggregate size of approximately 8:1.

4.2.5 Colored I-70/K-7 New ASTM Resistivity Results

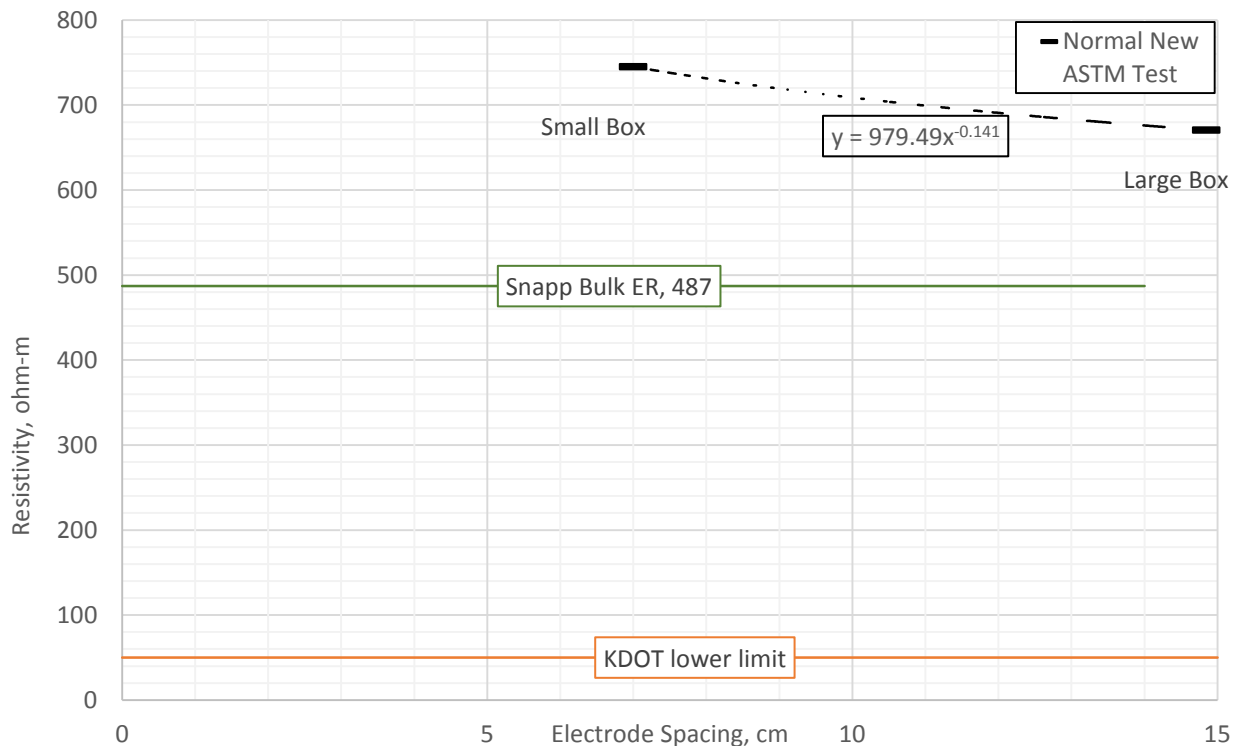


Figure 4.11: Colored I-70/K-7 New ASTM Results vs. Electrode Spacing

Figure 4.11 shows the resistivity of the Colored I-70/K-7 material as a function of electrode spacing. Five tests were conducted on the Colored I-70/K-7 material using the proposed ASTM procedure. Resistivity was so high, however, that just two results were obtained due to the NEMA, AASHTO, and Miller box resistance readings overloading the AEMC meter. The maximum calculable resistivity for the NEMA box was 422 ohm-m. The results still follow the trend seen in Figure 4.5e with respect to increasing electrode spacing lowering the resistivity result. The Snapp Bulk ER for dry I-70/K-7 compacted backfill resistivity was also very high, but was somewhat lower than either of the data points obtained in the lab.

4.2.6 New ASTM Testing Parameter Variations Results

Figure 4.12 shows the behavior of the calculated resistivity during draining, tilting and draining, and resting after draining for the SLT material in the NEMA and Large boxes. The jumps in resistivity seen at 16 minutes for the Large box and 21 minutes for the NEMA box were due to tilting at those times. The tilt angle for each box was approximately 10°.

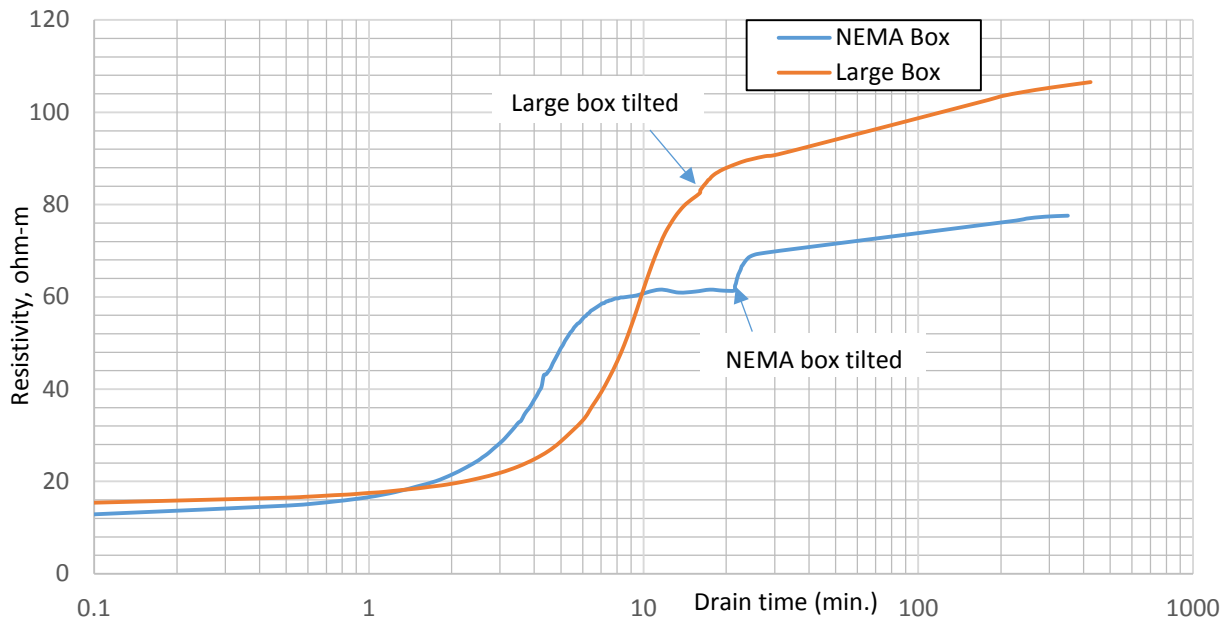


Figure 4.12: SLT Resistivity Behavior During and After Draining

The resistivity increased very slightly for the first few minutes as the box drained. It then began to increase rapidly as the water level approached the bottom of the box. An additional spike in resistivity occurred as the boxes were tilted to get the last of the freely draining water out of the box. The flow rate was much higher near the beginning of drainage and the effluent was mostly clear, which may have indicated a lower concentration of suspended sample particles. As the flow rate decreased, the effluent slowly turned a murky brown color, which may have indicated that more suspended solids were leaving the box than just after drainage started. Tilting the box also resulted in similar murky brown effluent. Resistivity continued to increase slightly over the next few hours after complete drainage.

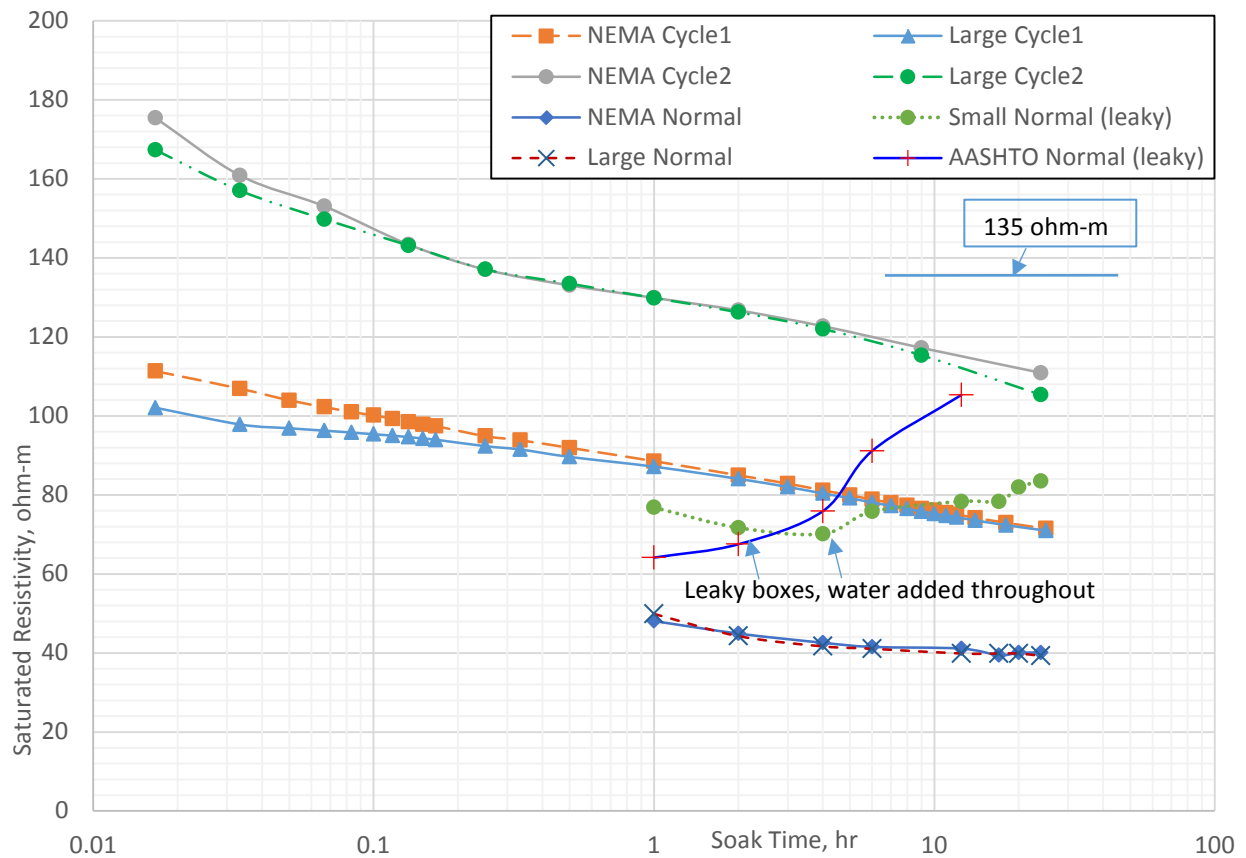


Figure 4.13: Pittsburg Cycled Saturated Resistivity vs. Soaking Time in Different Boxes

Figure 4.13 shows the calculated saturated resistivity changes for Pittsburg Cycle 1 and Pittsburg Cycle 2 materials in different boxes as functions of time spent soaking. Figure 4.13 shows a general trend of decreasing saturated resistivity with increasing soaking time for most data. The Large and NEMA box trends offer close correlation of saturated resistivity to the logarithm of soaking time. Equation 4.1 models this average correlation. This test was used to investigate the possibility of using a shorter soaking time in the New ASTM and then extrapolating the results to obtain the 24-hour result. This would allow a quick field test to either accept or reject MSE backfill before installation, rather than waiting on lab results for a 24-hour test if a saturated standard was adopted.

Both the Small box and the AASHTO box leaked substantially during this test, which required replacing about $\frac{1}{3}$ (2 inches) of the water in the Small box and $\frac{1}{2}$ of the water ($\frac{3}{4}$ inch) in the AASHTO box. Every time that battery DI water was added to these boxes, the resistivity increased. Considering that the added water was deionized, its addition must have diluted the concentration of ions that came from the sample.

Figure 4.14 shows the data from Figure 4.13 without the leaky boxes and with the drained resistivities of each cycle number of material in the Large box. The NEMA box, with its moderate box factor of 21.1 cm, contained the same material in a shape too resistive for the display of the AEMC meter.

Equation 4.1 is a best fit relationship for predicting the 24-hour resistivity of Pittsburg material based on any saturated resistivity result with soaking time between 10 and 1,440 minutes and is shown in Figure 4.14 plotted with the data from Figure 4.13. In addition, the similarity of the Large and NEMA results indicated that for saturated resistivity, the degree of repeatability of results across different box shapes was high, which suggests that these boxes were sufficiently large for box shape to not significantly influence resistivity.

$$R_2 = R_1 \left(\frac{t_1}{t_2} \right)^{0.057} \qquad \text{Equation 4.1}$$

R_2 = saturated material resistivity at desired soaking time (ohm-m)

R_1 = measured saturated resistivity (ohm-m)

t_1 = total soaking time elapsed for which R_1 was measured (hr)

t_2 = total soaking time elapsed for which R_2 is desired (hr)

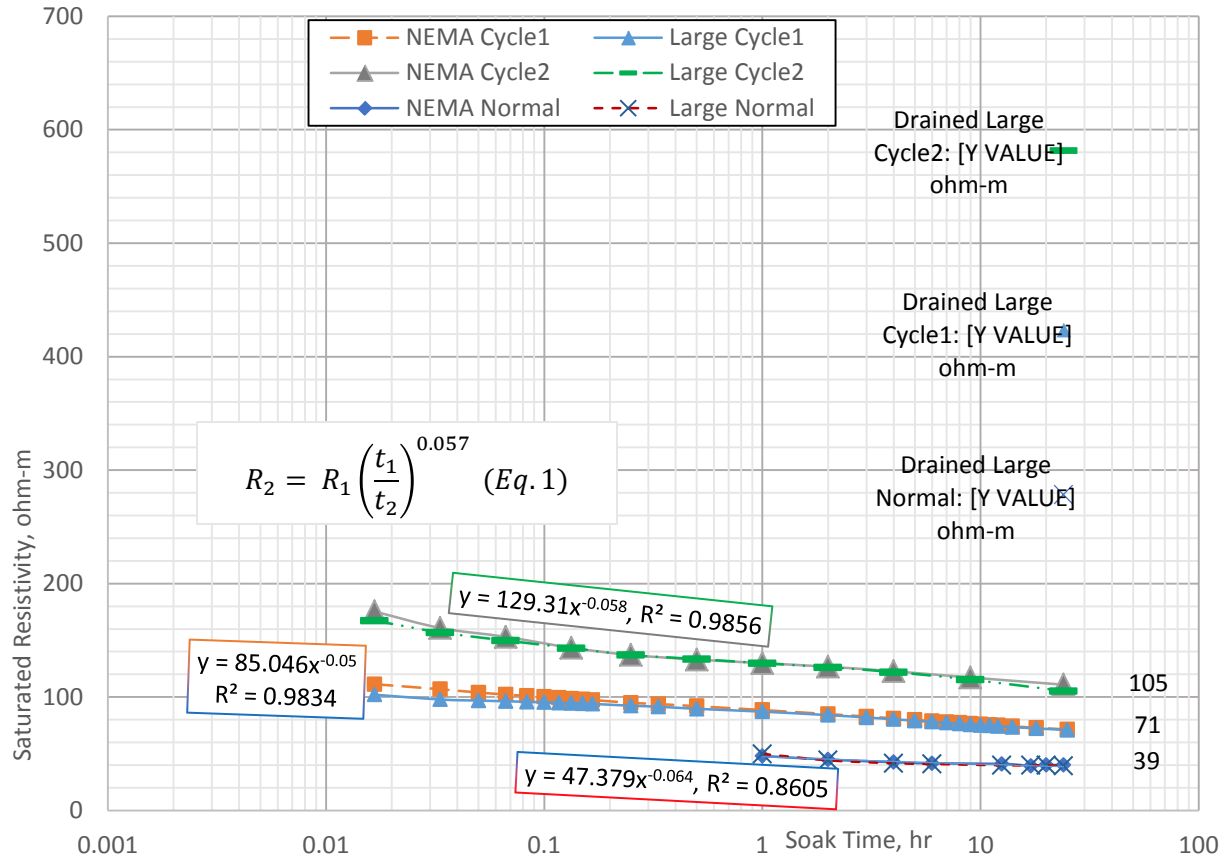


Figure 4.14: Pittsburg Saturated and Drained Cycled Resistivities vs. Soaking Time in Different Boxes

The saturated resistivity of the Pittsburg material increased substantially as it was drained and refilled and became Pittsburg Cycle 1 material, and also as Cycle 1 Pittsburg was drained and refilled and became Pittsburg Cycle 2 material. Figure 4.15 shows the drained resistivities of each of these different cycled materials.

Figures 4.14 through 4.16 show that increasing the number of soak/drain cycles of Pittsburg and Gray I-70/K-7 material generally resulted in increased resistivity. These cycles were intended to simulate rainfall events followed by drainage of the resulting pore water from the MSE backfill. Since resistivity increased as the number of cycles increased, the lowest resistivity for aggregate backfill may occur during the first rainfall/drainage event. Subsequent events appeared to result in increased resistivity. As Figure 4.16 shows, resistivity did not increase with increased cycles of Gray I-70/K-7 material for the two smallest boxes. The reason

for the lack of an increase in these small boxes is not well understood. One possible explanation is that this lack of resistivity increase with increasing soak-drain cycles in the Miller and AASHTO boxes may be related to the drainage method (vacuum drained) rather than gravity drainage. Drainage occurred through a much smaller opening and took much longer than for the larger, gravity drained boxes. This may have led to a smaller percentage of fines being removed during the drainage phase.

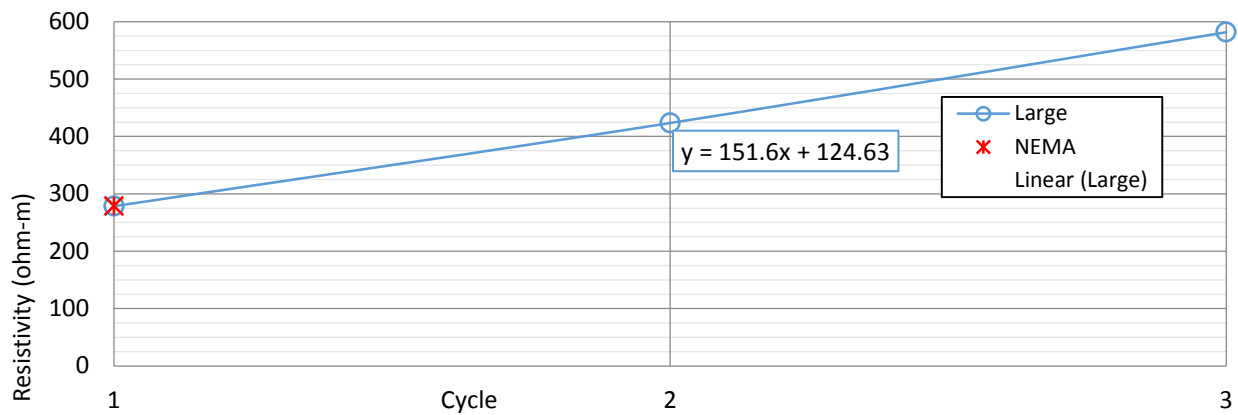


Figure 4.15: Cycled Pittsburgh vs. Drained Resistivity

Note: Same material as Figure 4.13

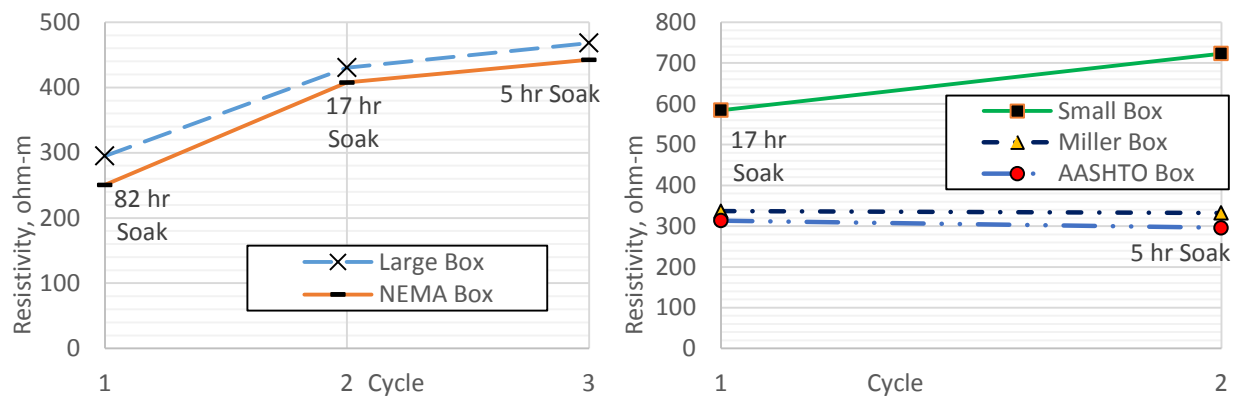


Figure 4.16: Cycled Gray I-70/K-7 vs. Drained Resistivity

Chapter 5: Conclusions and Recommendations

This report contains the results of a research study on the validity of the results of the AASHTO T 288 electrical resistivity test when applied to aggregates used as backfill for MSE walls. This AASHTO test and a proposed alternative ASTM test were used to test a set of aggregate samples obtained from MSE wall construction sites in eastern Kansas. Based on the results of this research, the following conclusions and recommendations were developed.

5.1 Conclusions

5.1.1 AASHTO T 288

Multiple issues were observed during the AASHTO T 288 tests. These include the maximum particle size limitation that may cause an unrepresentative sample to be tested, the water content used (supersaturated) likely to be unrepresentative of field conditions, and the cycling of the sample being tested that results in the loss of a significant percentage of sample solids and likely changes the sample composition to a condition less representative of field material.

The AASHTO test limits the maximum particle size to material passing the No. 10 sieve (2 mm). As Thapalia et al. (2011) reported, limiting an electrochemical test sample to a specific size fraction of an original sample can result in different measured electrochemical properties from those of the original sample. Thus, the limitation of particle size results in calculated resistivities that are representative of the material particles smaller than 2 mm in diameter, but may be unrepresentative of the aggregate as a whole. This tested fraction can be quite small. For the two aggregates tested with the AASHTO method in this study, compliance with the maximum allowable size required sieving 150 lb of each material to obtain the 1,500 g of sample necessary to run the test. The existing standard includes a note referring to its possible invalidity for aggregates with less than 5% passing the 2 mm sieve.

The AASHTO test often requires testing the aggregate sample in a supersaturated condition. It is very unlikely this condition will occur within significant portions of the backfill behind an MSE wall because MSE backfill should be designed to be freely draining.

Furthermore, if this condition did exist, then the wall would likely collapse due to the elevated water pressures behind it. There may be exceptions to this, such as the wall at the K-7 and I-70 interchange designed to permit water flow through the lower portions of the aggregate for periods of time. However, this particular wall has geosynthetic reinforcement.

A third issue with the AASHTO test is the requirement to continue cycling the material by emptying and cleaning the test box, mixing additional water into the sample, pouring all of the resulting slurry back into the box first, then adding sufficient solids back in to fill the rest of the box, and then testing until a minimum resistivity condition is reached. This procedure will change the sample being tested as solids are excluded from the tested portion of the sample during each cycle.

The AASHTO test and its corresponding box were originally designed for use with fine-grained material while the New ASTM test was developed with aggregate samples in mind. Thapalia et al. (2011) was one of the first to question the validity of the AASHTO method for aggregates. Yzenas (2014) was one of the first to actually propose a method to estimate the electrical resistivity of these aggregates that the AASHTO test specifically notes as possibly invalid for use with its procedure (i.e. aggregates with less than 5% passing the 2-mm sieve). Thus, this research investigated the applicability of the New ASTM proposed by Yzenas for use in determining the resistivity of aggregate backfills under field conditions.

5.1.2 New ASTM C XXX-XX

The New ASTM test and the existing AASHTO T 288 standard have considerable differences in procedures and results, and the new ASTM test appears to be more consistent with field conditions for the following reasons:

- The sample is allowed to drain. This should be representative of nearly all MSE wall backfill field conditions, except for special cases as noted previously.
- The full particle size range of the sample is used for the resistivity test and not just the fraction passing the No. 10 sieve (< 2 mm).
- There is not a cycling procedure that results in the exclusion of solids from the tested sample.

In addition to the points mentioned above, the box size adequate for the New ASTM will typically be much larger than the AASHTO box. This is important because if the aggregate sample material is to be tested with no size restriction, then the AASHTO box is almost certainly too small. A single large aggregate particle will often be taller than the AASHTO box and may span its width, and may therefore dominate current flow (and resistivity). There may also be resistivity measurement problems if the procedure is changed to allow the sample to drain. The drained sample will have a much higher resistance to current flow than the saturated sample. The resistance will be higher because the cross-sectional area of current flow is so small due to the reduced number of flow path options for the electrons to traverse the electrode spacing. This resistance is often too high to read using the AASHTO box with the standard meter recommended for AASHTO testing (as was the case for some conditions in this research), and a more sophisticated meter may be required to obtain useful results.

The New ASTM results for electrical resistivity exceeded those for the AASHTO standard by up to two orders of magnitude for the same aggregates. It is likely that this was primarily due to the gravity drained conditions for the New ASTM test versus the supersaturated conditions for the AASHTO test, although box size may have also played a role. Larger electrode spacing tended to yield lower resistivity values before leveling off above a certain value.

While conducting the New ASTM test on various samples using the different box sizes, several observations were made regarding possible issues and potential improvements to the procedure.

- The compaction procedure may not have ensured equal compaction efforts among the different box sizes, and so may have rendered the results of each box less comparable to one another for correlation purposes due to differing degrees of compaction.
- The lower value of the upper calculable resistivity limit of the Miller box due to its small size may limit its applicability to fine-grained soils.
- It may be necessary to develop a different acceptable minimum resistivity of aggregate backfills for corrosion purposes.

It is preferred that the box size be as small as practical for testing convenience. The similarity of the Large box and NEMA box resistivity curves for each Cycled SLT material in Figure 4.13 provided evidence of the ability to get consistent results from boxes with different shapes. Figures 4.5e through 4.7 and Figures 4.10 and 4.11 show that resistivity declined with increasing electrode spacing, although the additional decline above a certain spacing/aggregate size ratio was minimal (12:1 for SLT, 7:1 for Pittsburg, and 8:1 for Gray I-70/K-7).

Cycling tests were conducted on selected samples. For these tests the appropriately prepared and soaked sample was drained, the resistivity measured, the test box and same sample refilled with water, and the cycle repeated. This was done in an attempt to simulate the natural process of rainwater cycling through the aggregate. Electrical resistivity increased substantially for these samples with cycling as shown in Figure 4.13. This suggests that moving water through the backfill may “flush out” some of the constituents that promote current flow, and the resistivity may increase with time and with the number of rainfall then drainage events.

Covering the sample with a sheet of hard plastic while soaking was preferred to plastic wrap with a rubber band. Plastic wrap in contact with the sample and sample water was observed to draw significant amounts of pore water from the top of the sample out of the box via capillary action. For subsequent tests a hard plastic sheet was used to cover each box, and no further capillary action issues were observed.

Saturated resistivity was monitored during the soaking time of select samples and is seen in Figure 4.13. The saturated resistivity was shown to decrease as the samples soaked longer, so long as the box did not leak. The saturated resistivity of a longer soaking time for Pittsburg material could be predicted using Equation 4.1 (repeated below) based on a resistivity for a substantially shorter soaking time.

$$R_2 = R_1 \left(\frac{t_1}{t_2} \right)^{0.057} \qquad \text{Equation 4.1}$$

5.1.3 Comparison with Snapp Reported Bulk Field ER

The bulk ER reported for the SLT material was approximately 96.8 ohm-m (wet), which matches very well with the general values of the SLT Normal New ASTM results as shown in Figure 4.6. The bulk ER reported for the Ridgeview material was approximately 161 ohm-m (wet), which is higher than the general results from the Ridgeview Normal New ASTM results. This difference may be attributed to the failure of the Ridgeview material to drain properly via gravity during the New ASTM tests. The bulk ER reported for the combined Gray and Colored I-70/K-7 materials was approximately 487 ohm-m (dry), which is slightly higher than the New ASTM Gray I-70/K-7 results and lower than the New ASTM Colored I-70/K-7 results.

5.2 Recommendations

Based on the research conducted, it is recommended that KDOT consider replacing AASHTO T 288 testing with an alternative method, and that the New ASTM procedure be considered for adoption as it better reflects field conditions. As a part of this change, it is recommended that KDOT review the resistivity specification for aggregate backfills because it may need to be changed (increased) if a drained test is used instead of a saturated (or supersaturated) test.

It is recommended that adoption of a compaction method for the New ASTM similar to the Edlebeck and Beske (2014) method (predetermined unit weight) be considered to ensure equivalent compaction degrees across different box geometries.

Based on difficulties in water-proofing the edge-to-edge connections in the Small and Large boxes, it is recommended that a New ASTM test box be a single, molded shape of polycarbonate with four seamless sides connected with a seamless bottom and open top. It should have stainless steel electrode plates cut to match the inside dimensions of the desired sides for electrode plate installation and with constant side widths and heights along the sides and bottom of the box. Material types are recommended to conform to the AASHTO standard recommendations for test box material, electrode plate construction, and the fittings required to install the electrode plates and properly connect them to a resistivity meter.

The maximum particle size of the test material is used in the New ASTM to determine the minimum height of an appropriate test box. For this research the electrode spacing seemed to correlate most consistently with the resistivity of the material, and resistivity tended to decrease up to a certain electrode spacing (approximately 20 cm). Based on these results, an 8:1 ratio of minimum electrode spacing to maximum particle diameter is recommended on a preliminary basis. It is also recommended that the box height complies with the New ASTM recommendation of a 3:1 ratio of minimum box height to maximum particle size. It is also recommended that the box width perpendicular to the electrode spacing be reasonably consistent with the electrode spacing to promote a large number of aggregate contact points and current flow paths.

Based on the preliminary results of the variations of the New ASTM testing parameters, the New ASTM test soaking time may be shortened while still providing accurate results for saturated conditions. Research focusing on the applicability of Equation 4.1 to other MSE backfills is recommended. Further research into the effect of soaking time with more control over other parameters that affect resistivity such as degree of compaction, void ratio and porosity, water content, and mineralogy is recommended to accurately determine the minimum adequate soaking time for the New ASTM. Also, it is recommended that additional research be conducted to further explore the tentative relationships identified in this research between electrode spacing and other geometric box factors and resistivity in order to optimize the design of a New ASTM resistivity box.

References

- AASHTO T 27-14. (2014). *Standard method of test for sieve analysis of fine and coarse aggregates*. Washington, DC: American Association of State Highway and Transportation Officials.
- AASHTO T 288-12. (2012). *Standard method of test for determining minimum laboratory resistivity*. Washington, DC: American Association of State Highway and Transportation Officials.
- American Galvanizers Association (AGA). (2012). *Hot-dip galvanizing for corrosion protection: A specifier's guide*. Centennial, CO: Author.
- Association for Metallically Stabilized Earth (AMSE). (2006). *Reduced zinc loss rate for design of MSE structures: A white paper and proposal to change the metal loss model in the AASHTO specifications for design of MSE walls*. McLean, VA: Author.
- ASTM D75 / D75M-14. (2014). *Standard practice for sampling aggregates*. West Conshohocken, PA: ASTM International. doi: 10.1520/D0075_D0075M-14, www.astm.org
- Beckham, T.L., Sun, L., & Hopkins, T.C. (2005). *Corrosion evaluation of mechanically stabilized earth walls* (Report No. KTC-05-28/SPR 239-02-1F). Lexington, KY: Kentucky Transportation Center, College of Engineering, University of Kentucky.
- Billings, D.A. (2011). *Assessing corrosion of MSE wall reinforcement for I-15, Salt Lake County, UT* (Master's project). Brigham Young University, Provo, UT.
- Castillo, C., Hinojos, J., Bronson, A., Nazarian, S., & Borrok, D.M. (2014). Relating corrosion of mechanically stabilized earth reinforcements with fluid conductivity of backfill soils (Paper No. 14-3204). In *TRB 93rd Annual Meeting Compendium of Papers*. Washington, DC: Transportation Research Board.
- Edlebeck, J.E., & Beske, B. (2014). Identifying and quantifying material properties that impact aggregate resistivity of electrical substation surface material. *IEEE Transactions on Power Delivery*, 29(5), 2248-2253.

- Elias, V. (2000). *Corrosion/degradation of soil reinforcements for mechanically stabilized earth walls and reinforced slopes* (Report No. FHWA-NHI-00-044). Washington, DC: Federal Highway Administration.
- Esser, A.J., & Dingeldein, J.E. (2007). Failure of tieback wall anchors due to corrosion. In *Case studies in earth retaining structures* (Geotechnical Special Publication 159, pp. 1-10). doi: 10.1061/40903(222)4
- Low, G.P. (1895, February). Electrolysis and rail-bonding. *Transactions of the American Institute of Electrical Engineers*.
- Romanoff, M. (1957). *Underground corrosion* (National Bureau of Standards Circular 579). Washington, DC: U.S. Government Printing Office.
- Snapp, M.A. (2015). *Electrical resistivity measurements of mechanically stabilized earth retaining wall backfill* (Master's thesis). Kansas State University, Manhattan, KS.
- Thapalia, A., Borrock, D.M., Nazarian, S., & Garibay, J. (2011). Assessment of corrosion potential of coarse backfill aggregates for mechanically stabilized earth walls. *Transportation Research Record*, 2253, 63-72.
- Thornley, J.D., Siddharthan, R.V., Luke, B., & Salazar, J.M. (2010). Investigation and implications of mechanically stabilized earth wall corrosion in Nevada. *Transportation Research Record*, 2186, 154-160.
- Vilda, W.S., III. (2009). *Corrosion in the soil environment: Soil resistivity and pH measurements* (NCHRP Project 21-06). Washington, DC: National Cooperative Highway Research Program.
- Yzenas, J.J., Jr. (2014). New test method for measurement of aggregate resistivity using the two-electrode soil box method (ASTM WK24621). Submitted to ASTM Sub-Committee C-09.20, designation C XXX-XX.

Appendix A: Resistivity vs. Geometric Factors Other Than Box Factor

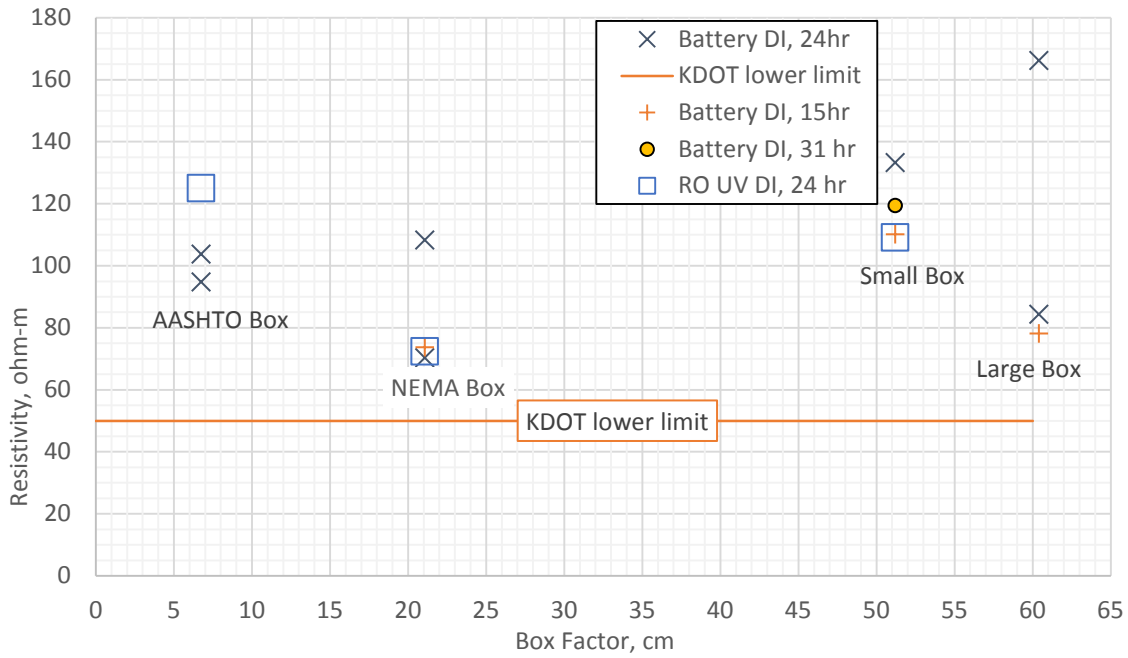


Figure A.1: New ASTM SLT Resistivity Results vs. Box Factor

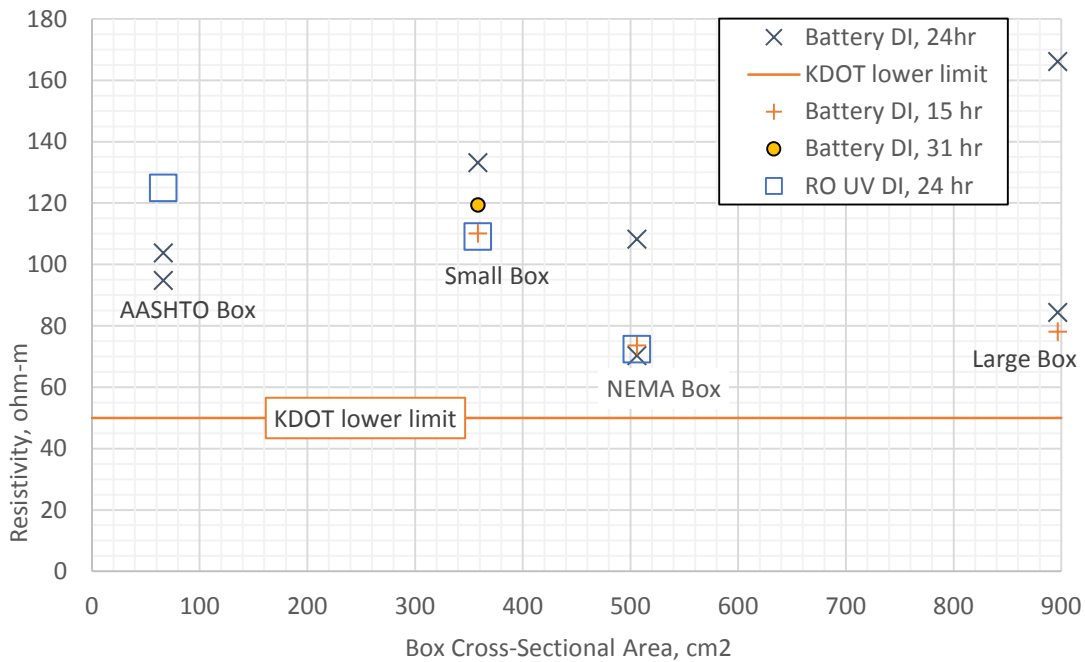


Figure A.2: New ASTM SLT Resistivity Results vs. Box Cross Sectional Area

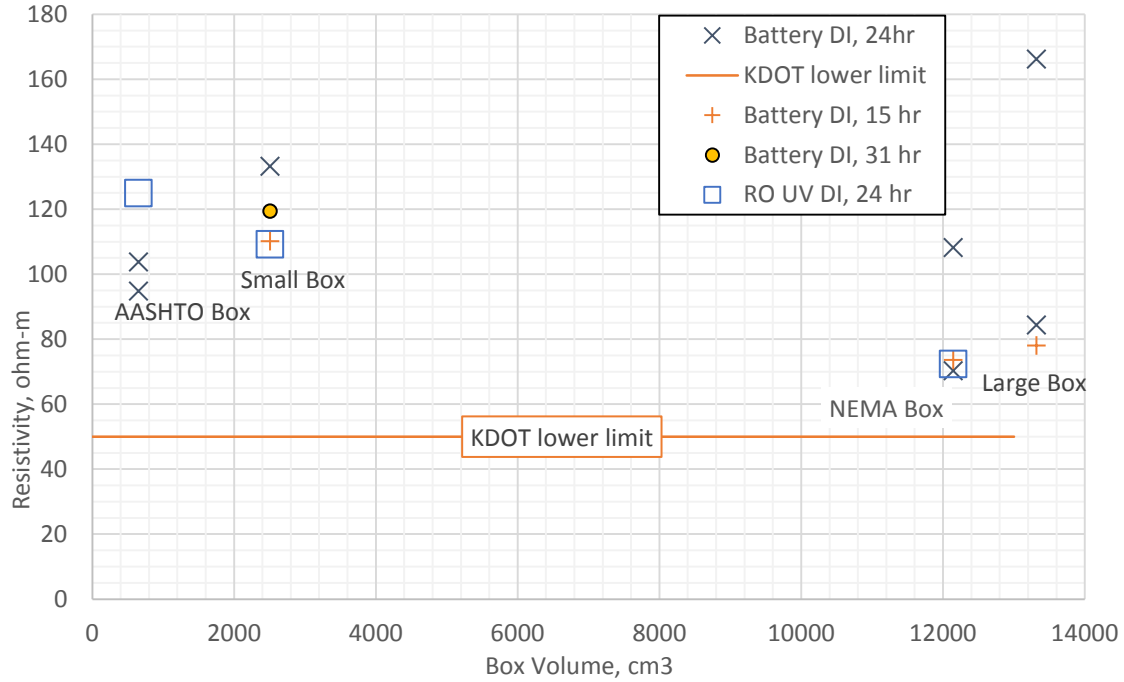


Figure A.3: New ASTM SLT Resistivity Results vs. Box Volume

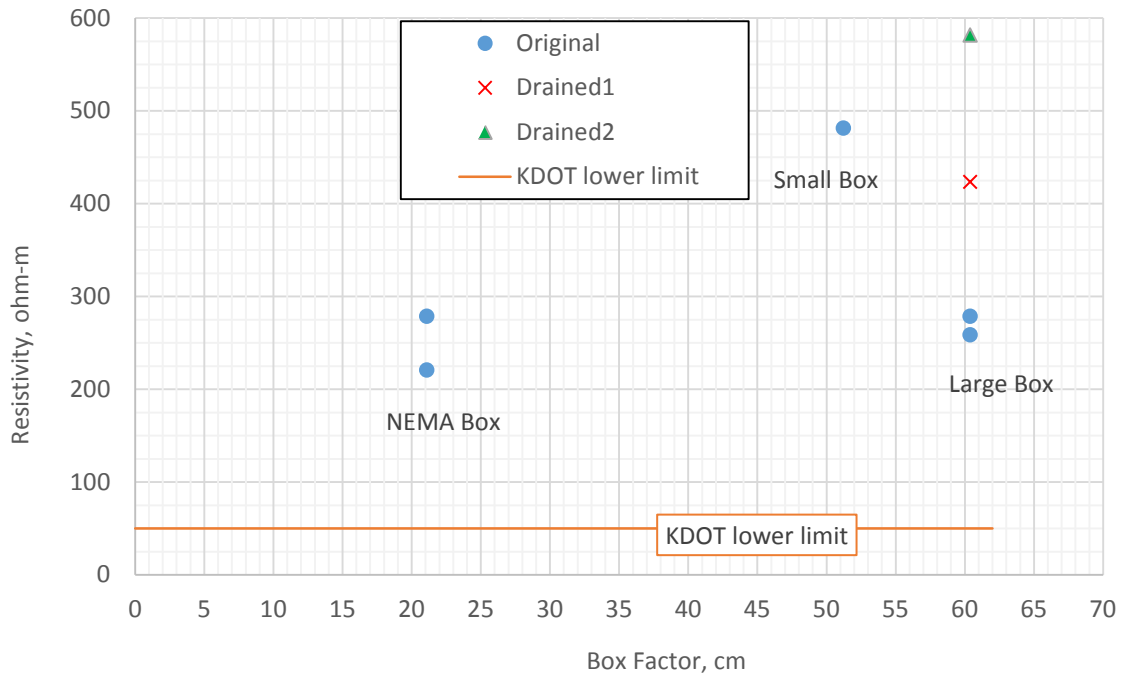


Figure A.4: New ASTM Pittsburg Resistivity Results vs. Box Factor

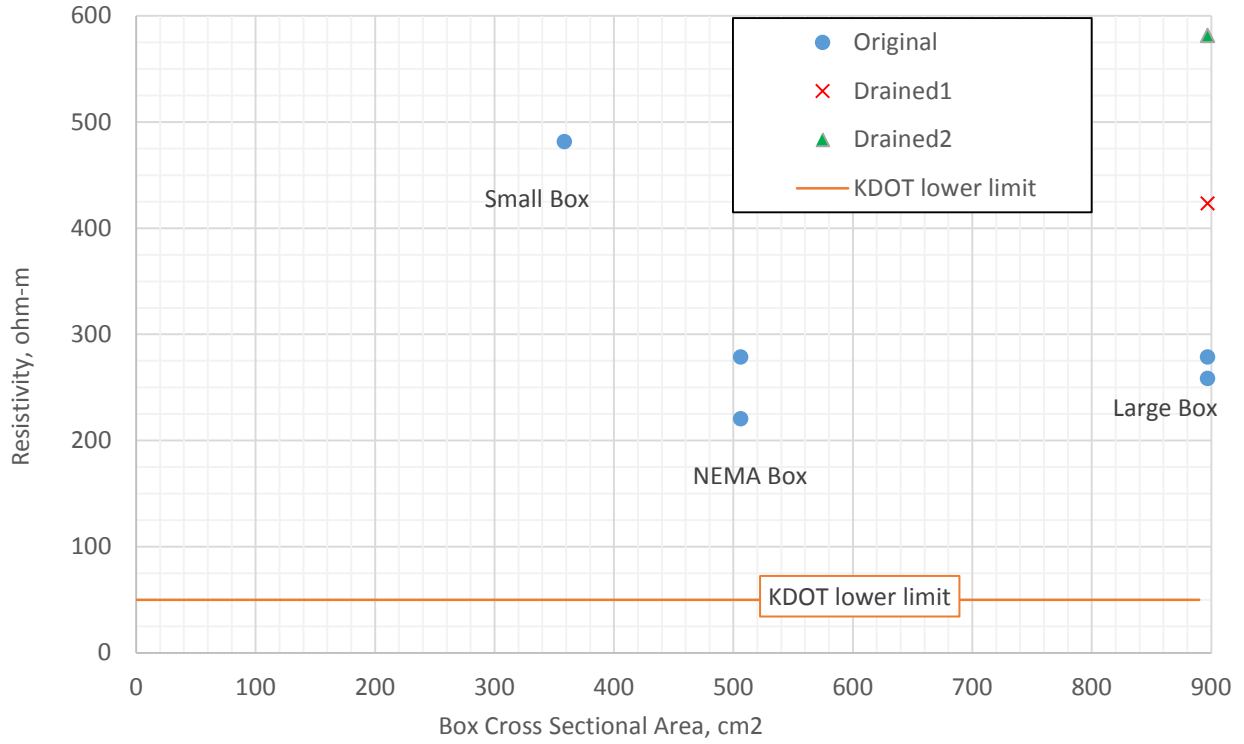


Figure A.5: New ASTM Pittsburg Results vs. Box Cross-Sectional Area

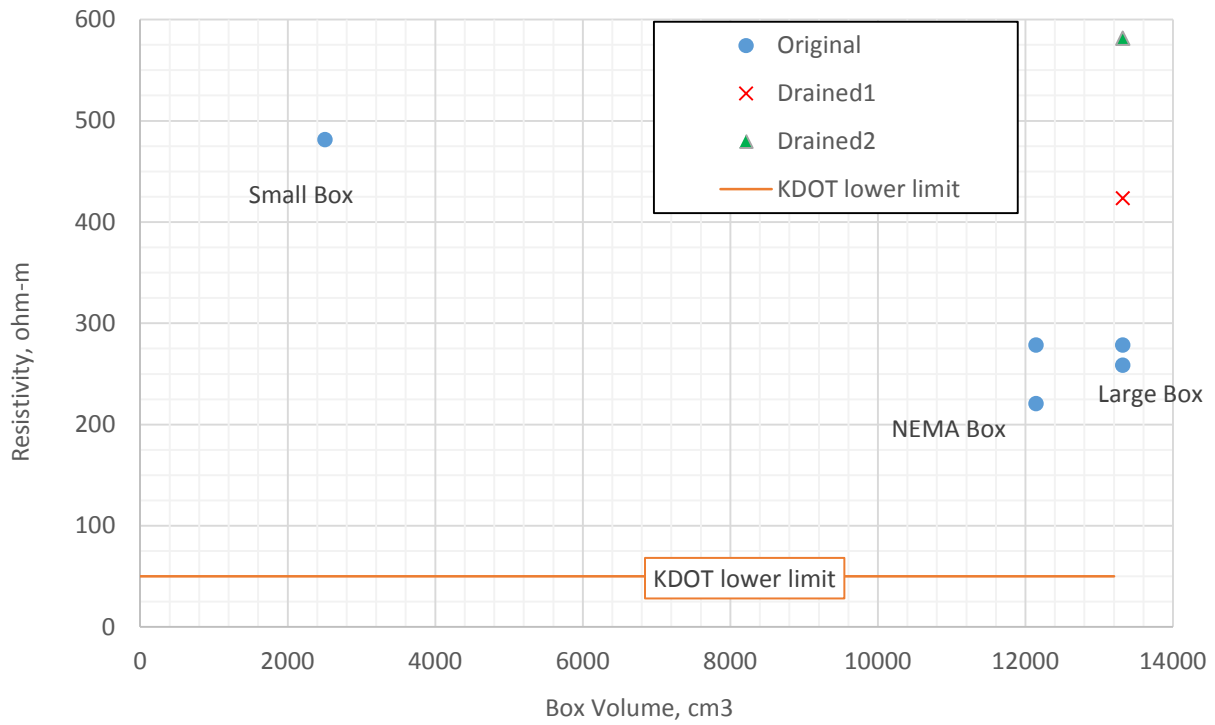


Figure A.6: New ASTM Pittsburg Results vs. Box Volume

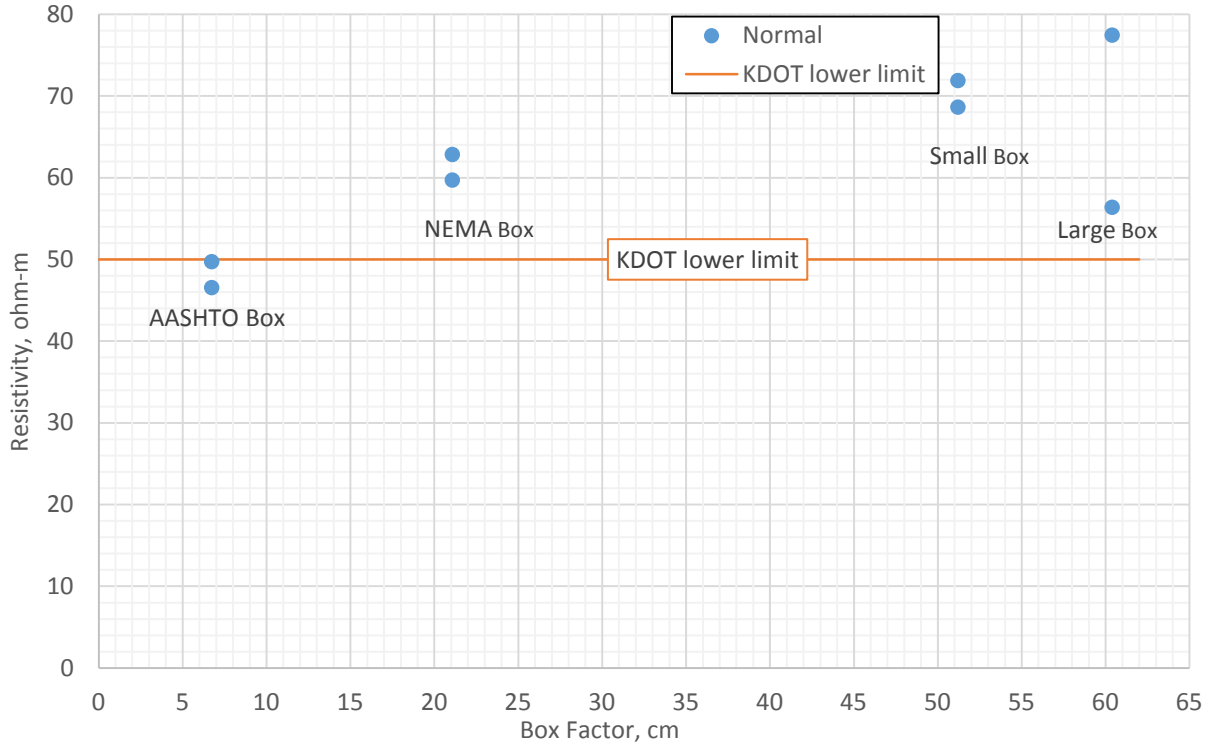


Figure A.7: New ASTM Ridgeview Resistivity Results vs. Box Factor

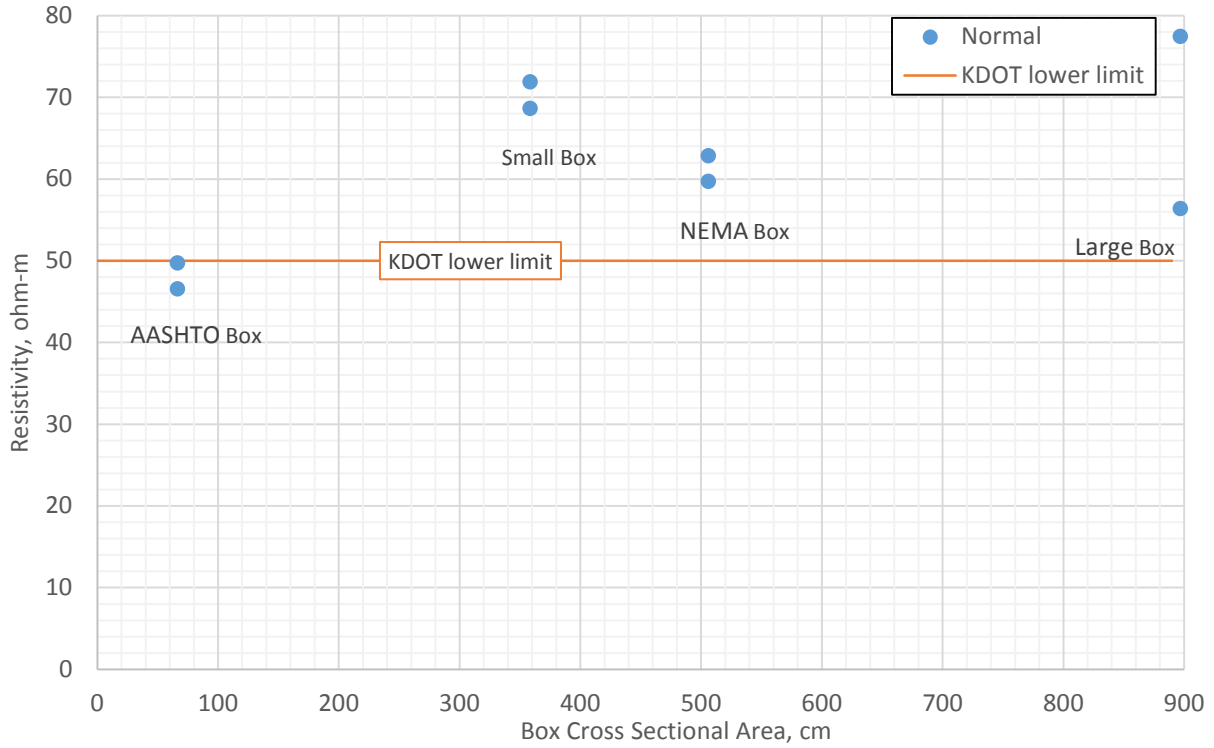


Figure A.8: New ASTM Ridgeview Resistivity Results vs. Box Cross Sectional Area

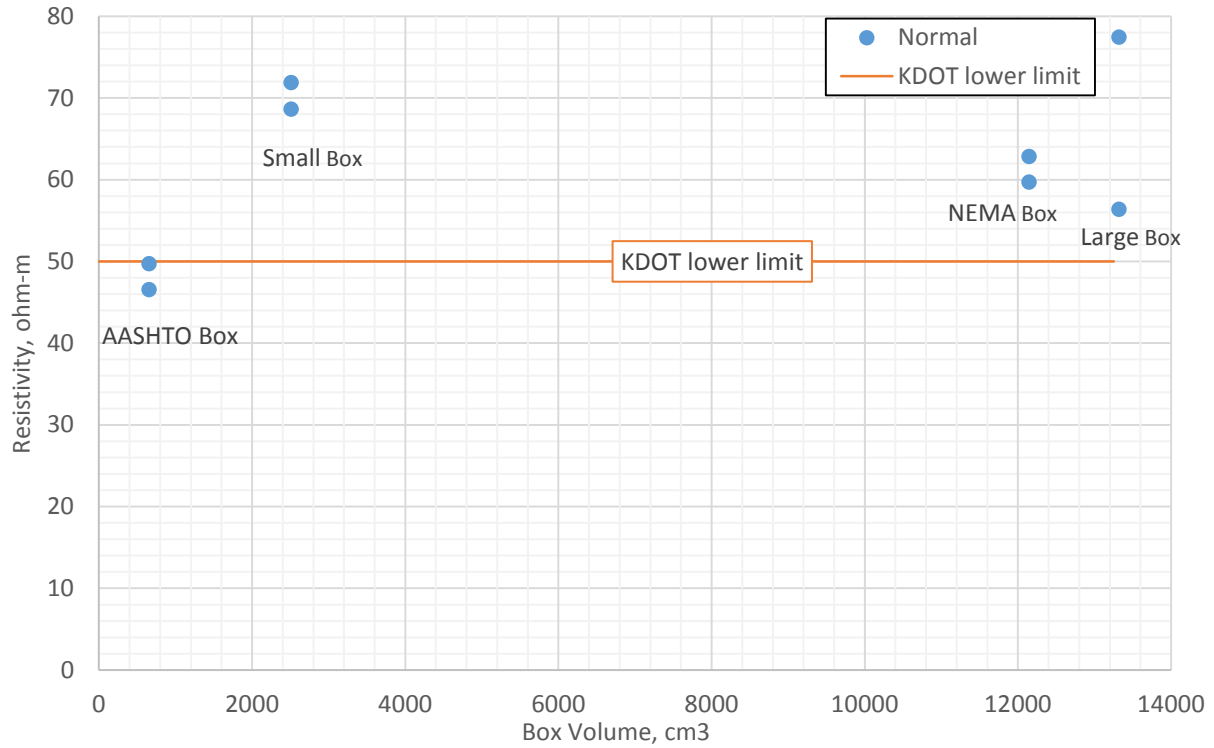


Figure A.9: New ASTM Ridgeview Resistivity Results vs. Box Volume

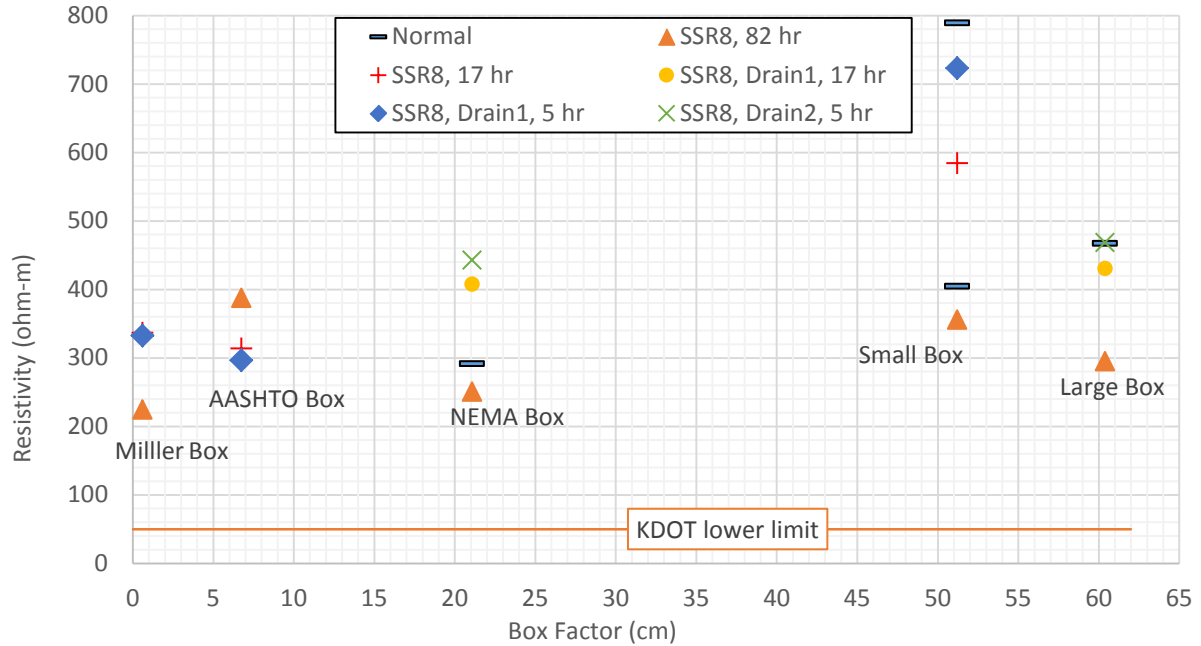


Figure A.10: New ASTM Gray I-70/K-7 Resistivity Results vs. Box Factor

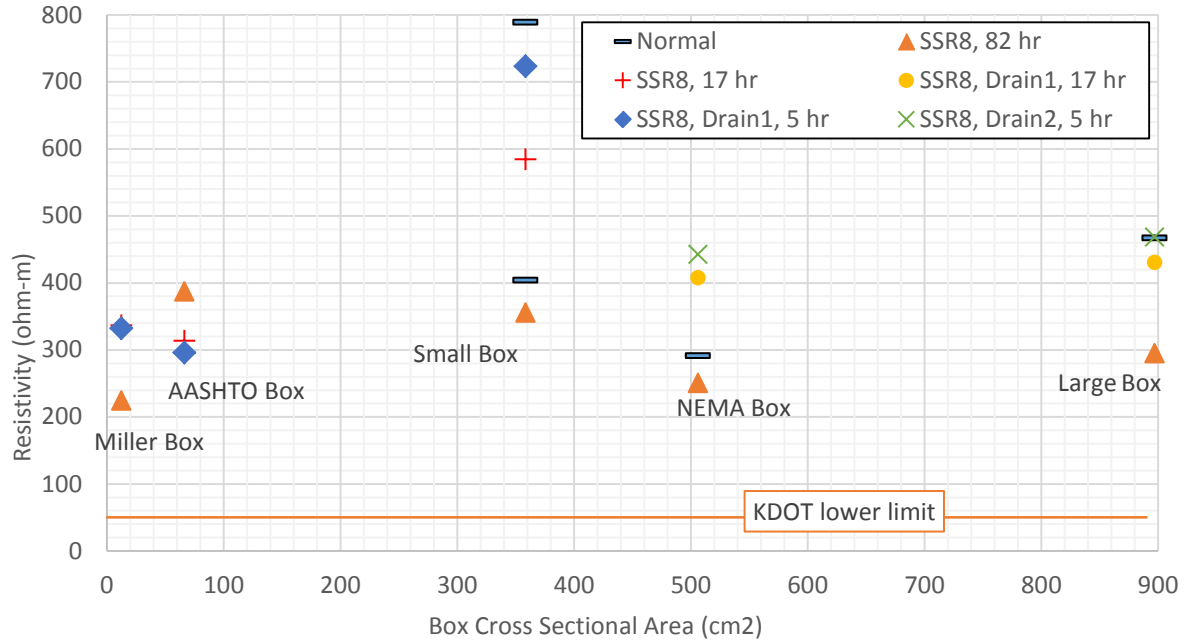


Figure A.11: New ASTM Gray I-70/K-7 Resistivity Results vs. Box Cross Sectional Area

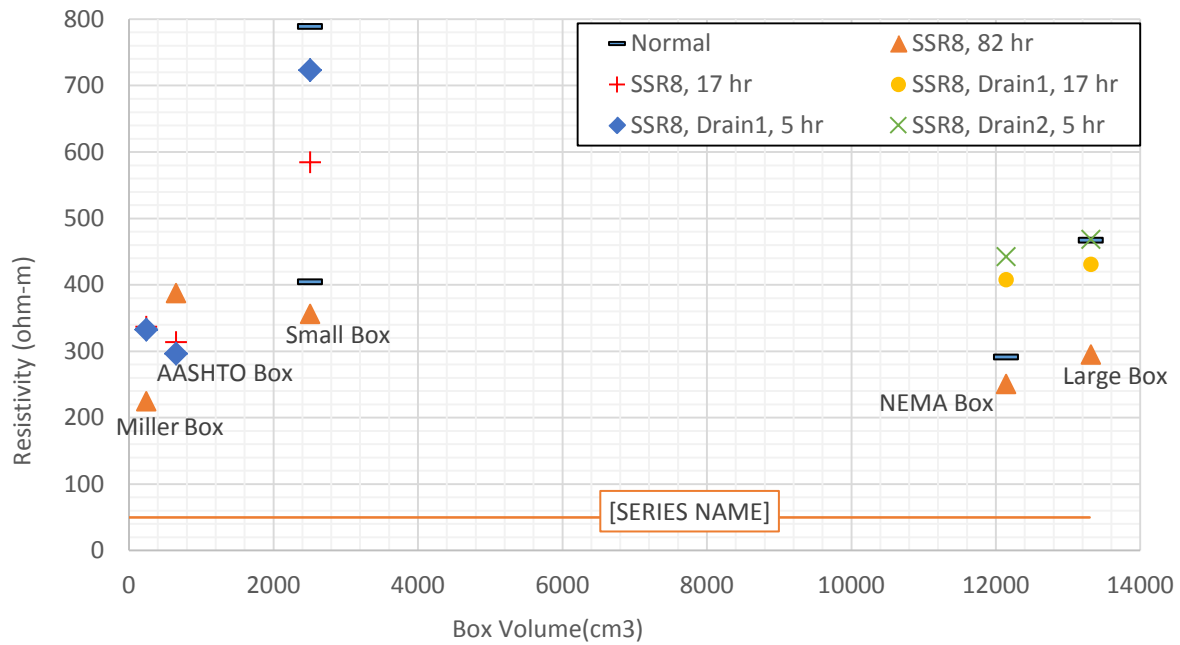


Figure A.12: New ASTM Gray I-70/K-7 Resistivity Results vs. Box Volume

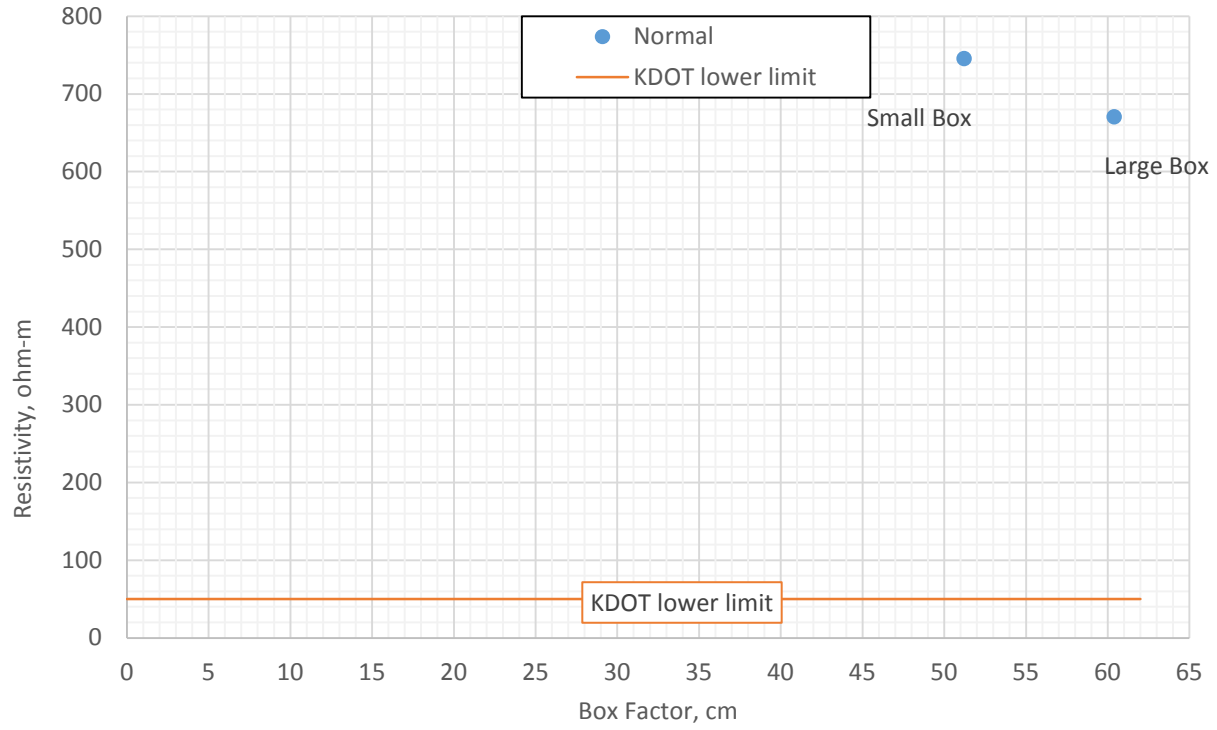


Figure A.13: New ASTM Colored I-70/K-7 Resistivity Results vs. Box Factor

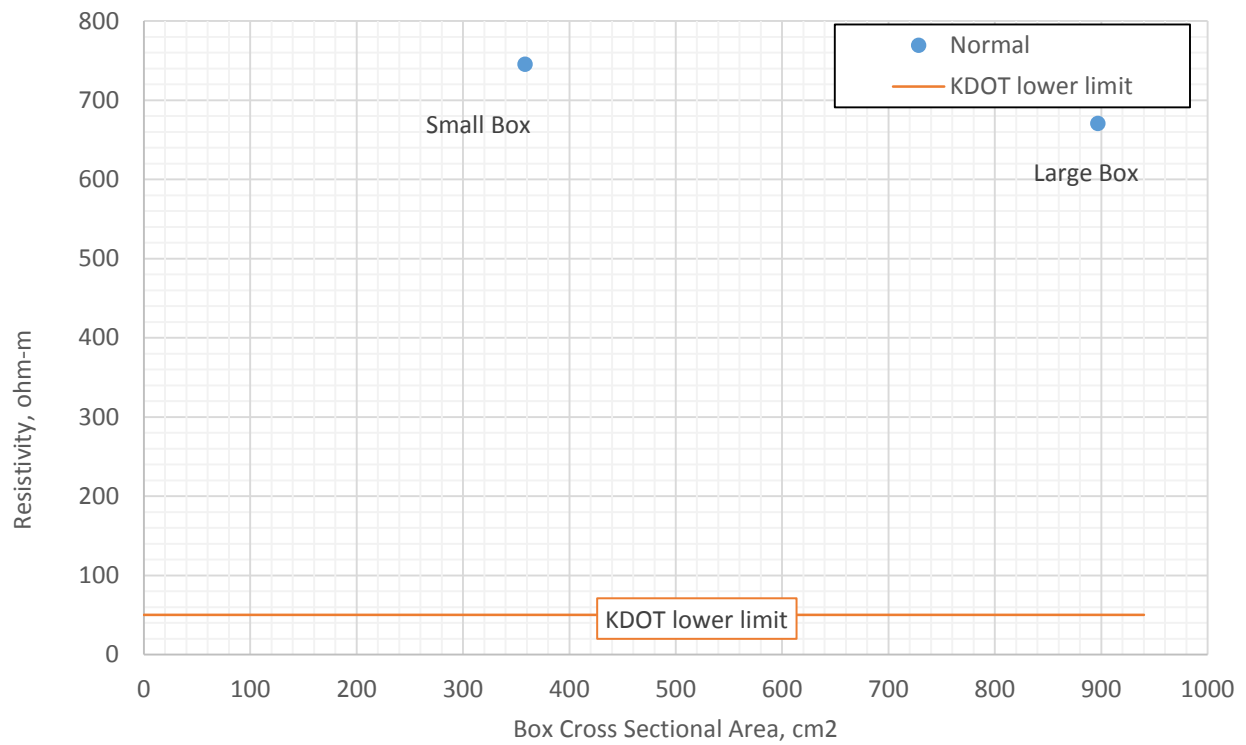


Figure A.14: New ASTM Colored I-70/K-7 Resistivity Results vs. Box Cross Sectional Area

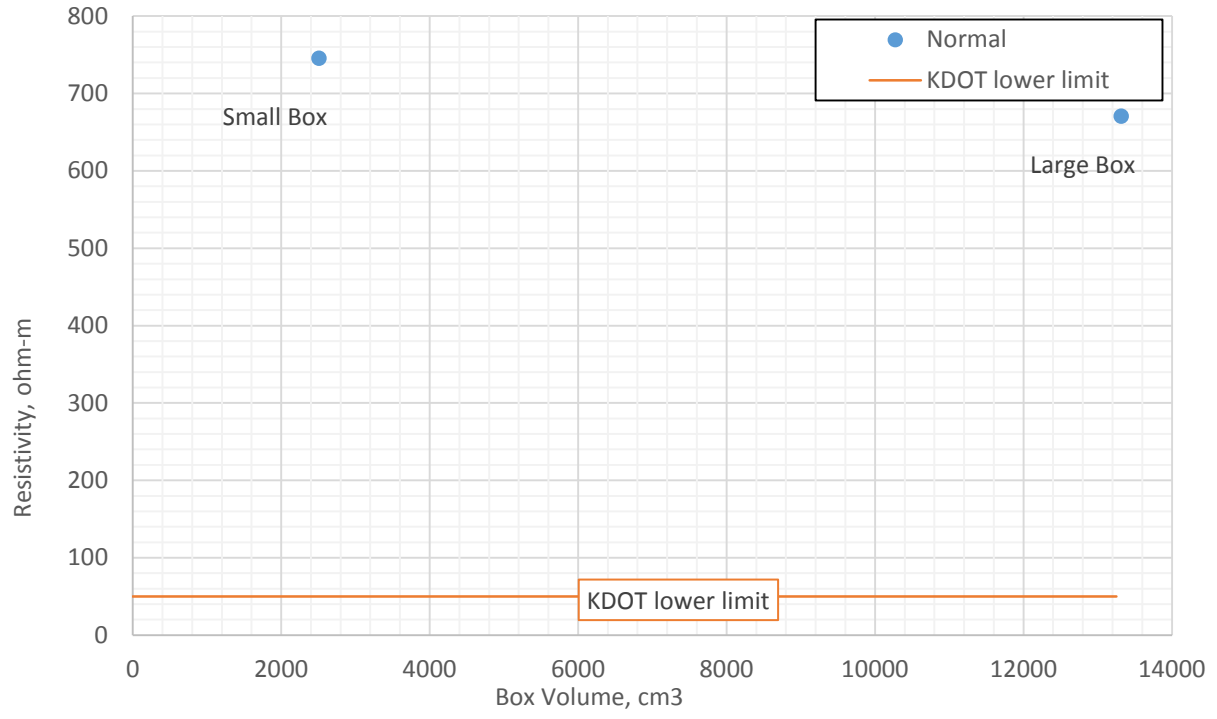


Figure A.15: New ASTM Colored I-70/K-7 Resistivity Results vs. Box Volume

K-TRAN

KANSAS TRANSPORTATION RESEARCH AND NEW-DEVELOPMENT PROGRAM

